
GEOPOLITICS, GEOFINANCIAL RISK: A MACHINE LEARNING APPROACH*

VERSION OF OCTOBER 2025

Alvaro Ortiz
BBVA Research & CRIW(NBER)
alvaro.ortiz@bbva.com

Tomaso Rodrigo
BBVA Research
tomaso.rodrigo@bbva.com

ABSTRACT

We introduce a novel high-frequency daily panel dataset of both markets and news-based indicators – including Geopolitical Risk, Economic Policy Uncertainty, Trade Policy Uncertainty and Political Sentiment – for 42 countries across both emerging and developed markets. Using this dataset, we study how sentiment dynamics shape sovereign risk, measured by Credit Default Swap (CDS) spreads, and evaluate their forecasting value relative to traditional drivers such as global monetary policy and market volatility. Our horse-race analysis of forecasting models demonstrates that incorporating news-based indicators significantly enhances predictive accuracy and enrich the analysis, with non-linear machine learning methods—particularly Random Forests—delivering the largest gains. Our analysis reveals that while global financial variables remain the dominant drivers of sovereign risk, geopolitical risk and economic policy uncertainty also play a meaningful role. Crucially, their effects are amplified through non-linear interactions with global financial conditions. Finally, we document pronounced regional heterogeneity, as certain asset classes and emerging markets exhibit heightened sensitivity to shocks in policy rates, global financial volatility, and geopolitical risk.

Keywords Geopolitics · Geoeconomics · Machine Learning · Shapley Values · Global Financial Cycle · News Indicators · Non Linearities · Heterogeneity

1 Introduction

Sovereign risk is a central concern for global financial stability, shaping borrowing costs, capital flows, and market resilience to economic and geopolitical shocks. Since the global financial crisis, and especially in recent years, heightened geopolitical and geoeconomic uncertainty has fueled interest in news-based text indicators such as Geopolitical Risk (Caldara and Iacoviello, 2022), Economic Policy Uncertainty (Baker et al., 2016), Trade Policy Uncertainty (Caldara et al., 2020), and measures of Political Sentiment (Ahir et al., 2018; Hassan et al., 2019). These indices capture high-frequency shifts in perceptions not fully explained by traditional fundamentals, and have been shown to affect investment, asset prices, and sovereign spreads (Novta and Pugacheva, 2021; Boubaker et al., 2023). Our objective is to examine empirically how such sentiment dynamics influences sovereign risk, as measured by the sovereign credit default swap (CDS) spreads.

To this end, we construct a novel daily panel dataset combining sentiment measures with conventional drivers such as U.S. monetary policy variables and global volatility proxied by the VIX index. We then conduct a comparative evaluation of machine learning (ML) models to identify the specifications that best capture the role of market and sentiment factors in sovereign-risk dynamics. Our approach builds on a growing literature highlighting the financial consequences of geopolitical and geoeconomic shocks, and extends it by embedding such factors in a unified sovereign risk framework.

A key objective is to assess how news-based indicators of geopolitical and economic uncertainty, when combined with traditional market variables, affect sovereign risk dynamics across countries. Specifically, we aim to evaluate

*The authors thank, without implicating, Stephen Hansen, Andreas Joseph and Martin Saldias. We especially thank to Buket Begün Boga, Patricia Soroa, Pablo Saborido and Ismael Frutos for their contribution to build the database.

their predictive power for sovereign CDS spreads and to test whether the inclusion of such high-frequency, sentiment-driven measures improves forecasting accuracy. By comparing linear and non-linear modeling approaches, we further seek to understand whether complex methods are better suited to capture the non-linearities and interdependencies that characterize the transmission of global shocks to sovereign risk. Moreover, we finally look for the presence of heterogeneity effects of the the main factors by asset class (developed and emerging) and emerging market regions.

The first contribution of the paper is the introduction of a novel and comprehensive high-frequency database of news-based indicators for 42 countries. This dataset allows us to test the relevance of text-based variables such as geopolitical risk, economic and trade policy uncertainty, and political sentiment jointly with traditional financial drivers like global policy rates and market volatility.

The second contribution is empirical. We show that news-based indicators markedly improve the forecasting accuracy of sovereign risk models, adding explanatory power beyond benchmarks based solely on financial and macroeconomic fundamentals. The gains are strong out of sample and depend on how the information is incorporated: linear specifications yield modest improvements, while non-linear methods such as Random Forests deliver the largest gains. This pattern suggests that the predictive value of news arises from non-linear interactions with financial variables, which standard linear frameworks—and particular reduction models as dynamic factor models—can underestimate.

The third contribution concerns methodology. We demonstrate that the information content of news variables is inherently nonlinear. Ensemble models, particularly Random Forest variants, are best suited to capture these dynamics. Our findings reinforce the view that uncertainty and geopolitical shocks affect sovereign risk through nonlinear channels, so that linear models risk missing key interdependencies, threshold effects, and complex spillovers (Hamilton, 1989; Teräsvirta, 1994; Rey, 2013; Gu et al., 2020; Joseph and Strobel, 2021; Bluwstein et al., 2023).

The fourth contribution is to highlight heterogeneity. We document cross-country and cross-market differences in how sentiment and global drivers affect sovereign risk. While global “push” factors remain central (Calvo et al., 1996; Rey, 2013; Miranda-Agrippino and Rey, 2020), their influence varies across advanced and emerging economies. Within emerging markets, Latin America, Asia, and Europe display distinct sensitivities linked to trade structures, institutional quality, and exposure to geopolitical risks (Didier et al., 2012; Reinhart et al., 2003; Fernández et al., 2018; International Monetary Fund, 2022; Bank for International Settlements, 2022). The Heterogeneity is not only present by asset class (Developed and Emerging) and geographical regions is also present for some factors between countries of the same group.

We address interpretability concerns by applying Shapley value-based explanations (Shapley, 1953; Lundberg and Lee, 2017). Shapley–Taylor interaction indices, and network analysis, which enable us to trace nonlinear interactions and variable importance in a transparent way. In doing so, we align with recent calls to use ML methods not as substitutes for structural models—but as complementary descriptive tools that uncover complex patterns and interactions in high-frequency data (Mullainathan and Spiess, 2017; Athey et al., 2018; Varian, 2014).

The paper proceeds as follows. Section 2 details our high-frequency database, combining traditional market variables with a suite of news-based sentiment indices. Section 3 introduces our machine learning framework and its application for model interpretation using Shapley values. Section 4 presents the main empirical findings, evaluating the predictive performance of the models and the insights from the Shapley value analysis including the interconnectedness analysis. Section 5 provides a factor decomposition for three major case studies: the Russia–Ukraine war, the Hamas–Israel conflict, and the geoeconomic shock from the shift in U.S. trade policy after Trump’s election. Section 6 concludes.

Related Literature

The determinants of sovereign risk have been studied through diverse lenses, including domestic fundamentals, global financial cycles, and the balance of “push” and “pull” factors. Within this broad field, our analysis highlights the role of news-based indicators—geopolitical, economic, and trade policy uncertainty—as complementary drivers of sovereign spreads. A growing literature shows that news signals convey timely information on risk, sentiment, and uncertainty, reinforcing traditional determinants. We extend this perspective by examining how news-based indicators interact with global financial cycle variables that feature prominently in work on external drivers of capital flows. In addition, we explicitly account for nonlinear dynamics in sovereign risk by employing machine learning models and Shapley value decompositions, which allow us to quantify the marginal contribution of distinct sources of risk. Our contribution thus connects to four strands of literature.

A first body of work develops has developed news-based measures of uncertainty and sentiment, including economic policy uncertainty (Baker et al., 2016), trade policy uncertainty (Caldara et al., 2020), and geopolitical risk (Caldara and Iacoviello, 2022). These indicators have been shown to influence investment, credit spreads, and asset prices (Hassan et al., 2019; Novta and Pugacheva, 2021), and have also been used to predict conflict and political violence

(Mueller and Rauh, 2018, 2022). We extend this literature by incorporating a broader set of high-frequency daily news-based indicators into sovereign risk models. Beyond economic and trade policy uncertainty and geopolitical risk, we integrate measures of economic sentiment, interest rate sentiment, and political tensions, providing a more comprehensive account of news-driven determinants of sovereign risk.²

Another strand examines Second, the literature on geopolitics and geoeconomics documents the financial consequences of conflict, sanctions, trade tensions, and global fragmentation. Geopolitical risk increases volatility and widens sovereign spreads (Fernandez-Villaverde et al., 2024; Boubaker et al., 2023), while trade tensions and sanctions amplify uncertainty and risk premia with potential effects on economic variables (Fernández-Villaverde et al., 2025; Ahn and Ludema, 2020; Aiyar et al., 2023; Benchimol and Palumbo, 2024). Our framework embeds these drivers in a unified empirical analysis of sovereign risk.

Third, this paper connects to the literature on the “push and pull” factors of capital flows and sudden stops (Calvo et al., 1996, 2004), as well as the Global Financial Cycle (Rey, 2013; Miranda-Agricuccio and Rey, 2020; Fratzscher, 2012), which highlights U.S. monetary policy and global financial volatility (VIX) as central drivers with significant effects on the real economy. Our contribution is to analyze these traditional global “push factors” jointly with domestic conditions, economic and trade policy uncertainty, and geopolitical risk. In doing so, we extend and confirm the predominant role of global financial variables while placing them in the broader context of new sources of risk.

Last, financial markets often display nonlinear dynamics such as threshold effects, asymmetries, and regime shifts (Hamilton, 1989; Teräsvirta, 1994; Cont, 2001). Recent work shows that ML methods can capture these complexities and improve prediction in crisis forecasting and risk spillovers (Gu et al., 2020; Joseph and Strobel, 2021; Bluwstein et al., 2023). Parallel literature highlights heterogeneity across countries, with advanced and emerging markets responding differently to global push factors (Calvo et al., 1996; Rey, 2013), and regional vulnerabilities shaped by institutions, trade structures, and financial integration (Didier et al., 2012; Reinhart et al., 2003; Fernández et al., 2018). Our contribution brings these strands together by using interpretable Machine Learning techniques to uncover nonlinearities and heterogeneous responses in sovereign risk.

2 The Data

This section provides a description of the high frequency daily database of country risk developed for the empirical analysis used in this work. The database integrates market-based financial indicators with news-based sentiment indicators to explain the performance of sovereign credit default swap (CDS) spreads, used as a proxy for sovereign credit risk, across 42 countries³.

All variables are first smoothed using a 28-day moving average to mitigate daily noise and isolate persistent trends. Subsequently, each series is standardized to have a zero mean and unit variance over its respective sample period for each country. Our analysis uses an unbalanced panel spanning from January 2017 to July 2025; Country-specific data availability, as well as percentile distributions by country, are detailed in Appendix A. This pre-processing ensures comparability across indicators while preserving the informational content of large shocks. Consistent with this objective, we do not perform any outlier treatment, as we consider extreme events to be informative signals of exceptional shifts in risk perception.

Our main contribution in the dataset is the construction of coverage and sentiment-based measures on daily basis derived from international news sources for some of the explanatory variables. These indicators are produced by BBVA Research using the *Global Database of Events, Language, and Tone (GDELT)*, an open-source platform that monitors and parses global digital media⁴ Leetaru and Schrodt (2013), GDELT covers broadcast, print, and online outlets in more than 100 languages, updated every fifteen minutes, and provides a high-frequency and wide-coverage record of events worldwide. Articles mentioning relevant topics are identified in their local language, translated into English

²These daily indicators are updated weekly at BBVA Research. We also provide evidence on their relevance and heterogeneity relative to traditional determinants of country risk.

³The included countries in the analysis are Argentina, Australia, Austria, Belgium, Brazil, Canada, Chile, China, Colombia, Czech Republic (CzechRep), Denmark, Egypt, Finland, France, Germany, Hungary, India, Indonesia, Israel, Italy, Japan, Jordan, Malaysia, Mexico, Morocco, Netherlands, Norway, Peru, Philippines, Poland, Qatar, Russia, Saudi Arabia, Sweden, Spain, Thailand, Turkey, Ukraine, United Kingdom, United States, Uruguay and Vietnam. The countries are classified by region too.

⁴An alternative, and widely used, source for constructing such news-based indicators is the Dow Jones Factiva database. Unlike the open-source GDELT platform, Factiva is a premium, subscription-based archive that provides access to a vast and deeply curated collection of licensed global news sources, news-wires, and trade publications. Its extensive historical data and high-quality sources make it a common choice in academic research for building custom, long-run indicators. For example, the historical component of the widely-cited Economic Policy Uncertainty (EPU) index is constructed using news archives from Factiva.

and processed applying a vast amount of algorithms to create indicators based on total media, foreign media and local sources.

Following Bondarenko et al. (2024), we rely on local media sources rather than foreign media to construct the indicators. Local newspapers provide a more accurate representation of risks and uncertainties are perceived domestically. Bondarenko et al. (2024) captures, for geopolitical risk, heterogeneity in national perspectives, proximity to conflict, and differences in press coverage that global (English-language) media often miss. They show that shocks identified from local news sources have significant effects on domestic financial markets and macroeconomic conditions, whereas shocks based on Anglosphere media tend to underestimate local impacts.

We construct two types of news-based indicators. The first type measures "*Uncertainty*" and is based solely on the volume of relevant news coverage. For our Economic and Trade Policy Uncertainty indices, we follow the methodology in line with the original methodology Baker et al. (2016). Specifically, we compute coverage as the daily share of articles containing a predefined set of uncertainty-related keywords, with the complete keyword lists detailed in the Appendix A. This measure is then normalized by the total volume of daily news for each country to create a robust indicator that accounts for secular trends in media output and processing noise.

The second type of indicator combines *News Volume and Sentiment*. This approach is used to construct our indices for domestic Economic Sentiment (ECO), Local Interest Rate Sentiment (INT), Geopolitical Risk (GPR), and Political Tensions (POL). For these variables, we first compute the average sentiment of all relevant articles. This is achieved by scoring the text with over 40 different GDELT sentiment dictionaries, yielding a tone score typically ranging from -10 (highly negative) to +10 (highly positive). The final index is then the product of this sentiment score and the normalized news coverage. This product is inverted for interpretability, ensuring that a higher index value consistently corresponds to greater risk or more negative sentiment.⁵

The dependent variable is the sovereign credit default swap (CDS) spread. A sovereign credit default swap (CDS) is a derivative contract in which investors pay a premium to insure against credit events—default, restructuring, or missed payments—on a sovereign’s external, foreign-law bonds. The CDS spread is thus an option-implied measure of sovereign default risk. CDS spreads reflect the cost of insuring against a sovereign default, which are widely used as a market-based measure of sovereign credit risk. CDS spreads provide a comprehensive indicator of how markets assess sovereign risk at a given point in time.

The set of the explanatory variables to explain the sovereign risk fluctuations are included in three groups of variables, representing the global financial conditions, the domestic situation and political and geopolitical framework⁶ :

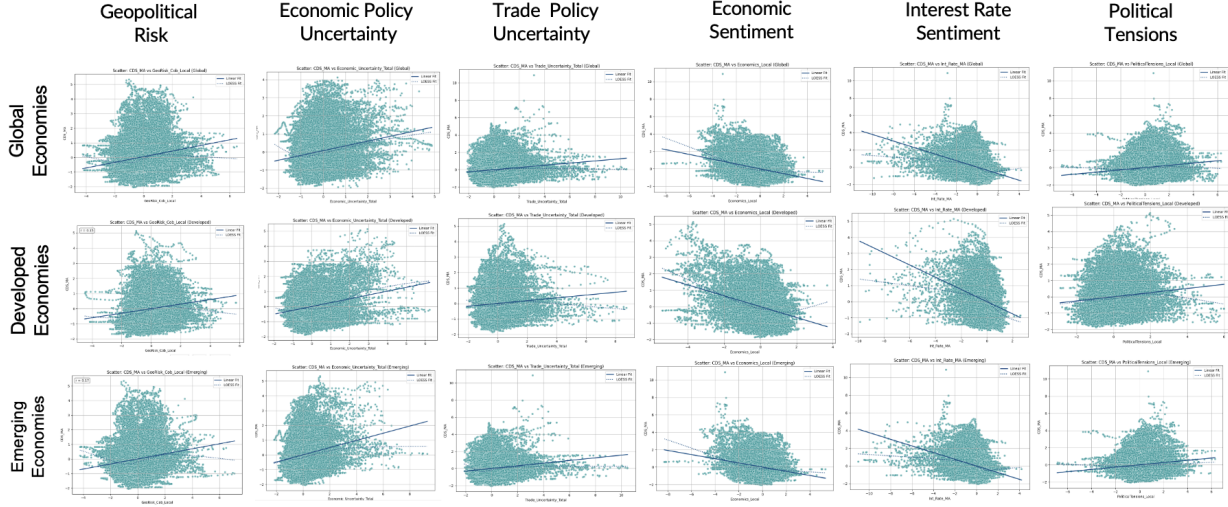
- Global Financial Variables. To capture global financial conditions, we rely on market data for two key variables, representative of global monetary policy and global volatility:
 - *Federal Reserve Policy Rate (FED)*. To avoid the zero policy rate of the federal reserve, we rely on the 2 years yield as suggested by Swanson (2021) the 2-year US Treasury yield to reflect the cost of government borrowing in the financial market.
 - *Global financial volatility (CBOE Volatility Index, VIX)*, which measures implied volatility in the S&P 500 and is commonly referred to as a “fear index,” capturing shifts in global investor risk aversion.
- Macroeconomic sentiment variables. We develop some media-based sentiment indicators about domestic economic activity, monetary policy and economic and trade uncertainty:
 - *The Economic Sentiment Indicator (ECO)* captures the narrative framing of the broader economic environment, as perceived by society, investors, and policymakers, reflecting the narratives and expectations that shape market behavior.
 - *The Interest Rate Sentiment Indicator (INT)*, that reflects perceptions and expectations regarding monetary policy and borrowing costs, quantifying expectations and narratives around monetary policy.
 - *The Local Economic Policy Uncertainty (EPU) Index*, which captures references to ambiguity regarding economic policy decisions in the media.
 - *The Trade Policy Uncertainty Index (TPU)*, which focuses on uncertainty related to international trade rules, negotiations, and disputes.

⁵A detailed description of the keyword sets, dictionaries, and construction formulas for all indicators is provided in the Appendix A. The complete set of daily and weekly indicators is publicly available at our online dashboard: <https://bigdata.bbvaresearch.com/en/>.

⁶Existing work emphasizes structural determinants of external debt dynamics. Our contribution is complementary: we incorporate high-frequency, news-based indicators alongside global financial conditions, domestic macroeconomic settings, and political–geopolitical tensions, all of which bear directly on sovereign default risk.

- *Political and Geopolitical Sentiment variables.* To track political tensions and geopolitical risks, we construct Geopolitical Risk indices as well as Political Risk Sentiment indices, described as following:
 - *The Geopolitical Risk Index (GPR)* reflects the prevalence of international conflict, military disputes, and terrorism.
 - *The Political Tensions Indicator (POL)* emphasizes domestic instability, unrest, and political contestation.

Figure 1: Scatterplots of Uncertainty & Sentiment vs Risk (Linear & Non-Linear fit)



Notes: Figure 1 plots sovereign CDS spreads against six categories of uncertainty and sentiment measures: Geopolitical Risk, Economic Policy Uncertainty, Trade Policy Uncertainty, Economic Sentiment, Interest Rate Sentiment, and Political Tensions. Columns correspond to each category, while rows distinguish between Global, Developed, and Emerging Economies. Both linear (solid line) and locally weighted scatterplot smoothing (LOESS; dashed line) fits are included. The results indicate a generally positive relationship between uncertainty indices and sovereign risk, and a negative association for sentiment measures, with magnitudes varying across economies. The link between uncertainty and risk is particularly pronounced in emerging markets.

Figure 1 presents the scatterplots of sovereign risk or CDS spreads against the set of news-based variables: uncertainty measures including the Economic Policy Uncertainty (EPU), Trade Policy Uncertainty (TPU) and sentiment indicators as Economic Sentiment (ECO), Interest Rate Sentiment (IRS), Geopolitical Risk (GPR) and Political Tensions (POL). The plots are shown for global, developed, and emerging economies, with both linear and non-linear fits.

Overall, the figures highlight that all of the variables have the correct not significant sign and the heterogeneous and often non-linear nature of the relationship between sentiment, uncertainty, and sovereign risk. Economic and trade policy uncertainty display weak but positive associations with risk, particularly for emerging markets, suggesting that higher uncertainty is accompanied by rising CDS spreads. By contrast, the sentiment indicators exhibit clearer patterns: negative economic and interest rate sentiment are strongly associated with higher risk premia, with the relationship being sharper in developed economies. Geopolitical risk shows a weaker linear pattern but displays visible non-linearities, consistent with the idea that geopolitical shocks matter primarily during periods of heightened stress. Political tensions reveal weaker explanatory power, with wide dispersion across economies.

Taken together, the scatterplots provide preliminary evidence that while traditional uncertainty measures play some role, sentiment variables—especially those related to macroeconomic and financial conditions—are more closely aligned with sovereign risk dynamics. The stronger fits observed in emerging markets further suggest that these economies are particularly sensitive to news-based indicators.

3 Methodology: Assessing the Impact of News Based Sentiment on Risk

This section outlines our empirical strategy for assessing how high-frequency, news-based sentiment and uncertainty shape sovereign risk, measured through credit default swaps (CDS). We begin with a *machine-learning horse race*—spanning linear and regularized regressions, tree-based methods, and neural networks—to compare predictive

performance using only information available up to each forecast origin. The horse race identifies the best-performing model out of sample, which we then hold fixed for interpretation. To address the “black box” critique, we apply Shapley value decompositions Lundberg and Lee (2017) to trace how different drivers contribute to sovereign risk over time and to build narratives around key episodes, such as geopolitical shocks or shifts in global financial conditions. Finally, we examine cross-country transmission through two complementary interconnectedness metrics—Diebold–Yilmaz spillovers Diebold and Yilmaz (2014) and a nonparametric network-density measure—which allow us to distinguish directional propagation from synchronous co-movement.

3.1 A Machine Learning Horse Race Approach

This section examines how news-based measures of uncertainty and sentiment shape sovereign risk. Departing from models centered on low-frequency structural fundamentals, our analysis focuses on high-frequency market and news indicators that capture the drivers of country risk: global financial conditions, economic and trade policy uncertainty, sentiment regarding macroeconomic and interest-rate conditions, and geopolitical or political risks. Sovereign risk is proxied by standardized credit default swap (CDS) spreads for 42 countries, demeaned and normalized to highlight deviations from country-specific norms and facilitate cross-country comparability. Building on the data framework described above, we hypothesize that sovereign risk reflects the joint influence of global financial variables (e.g., policy rates and the VIX), domestic macroeconomic, economic and trade policy uncertainty and political–geopolitical tensions.

To evaluate this hypothesis, we consolidate these drivers into a predictor vector $\mathbf{X}_{i,t}$ for country i at time t , and assess their predictive content within a range of models. Identifying the true form of $f(\cdot)$ is challenging, specially when the relationship between the dependent and independent explanatory variables may be highly nonlinear (Varian, 2014; Mullainathan and Spiess, 2017). Standard linear models are ill-suited to capture threshold effects, interactions with fundamentals, or saturation. To avoid imposing restrictive functional assumptions, we adopt a *machine learning horse race* that compares a wide range of model classes.

$$y_{i,t+1} = f(\mathbf{X}_{i,t}, \boldsymbol{\lambda}_i) + \varepsilon_{i,t+1}, \quad (1)$$

where $\boldsymbol{\lambda}_i$ are geography dummies capturing country-specific fixed effects.

The objective of the *horse race* is to identify the model class that achieves the best predictive performance in a pseudo–real time setting,⁷ where forecasts are generated recursively using only information available up to period t . Predictive accuracy is evaluated by minimizing a loss function of out-of-sample forecast errors. Formally, given errors $e_{i,t}^{(m)}$ from model m , the estimator is defined as:

$$\hat{f}^{(m)} = \arg \min_{f \in \mathcal{F}_m} \mathcal{L}^{(m)} = \frac{1}{|\mathcal{S}|} \sum_{(i,t) \in \mathcal{S}} L(e_{i,t}^{(m)}), \quad (2)$$

where \mathcal{F}_m is the model class (e.g., linear, penalized linear, tree-based), and $L(\cdot)$ the chosen loss function (e.g., out-of-sample mean absolute or root mean squared error).

A key concern is to avoid contamination between training and test samples. Because we work with time-series data in an unbalanced panel, standard random-sample splits used in cross-sectional machine learning are inappropriate. Instead, we adopt a recursive forecasting framework, which re-estimates models using only past data and produces out-of-sample forecasts that preserve the chronological order, thereby avoiding look-ahead bias. Moreover, since variables are measured as 28-day moving averages, observations near train–test cut-offs risk overlap. To prevent leakage, we impose a 28-day buffer around each split, ensuring that training and test sets remain strictly separated.

The empirical procedure is as follows. First, models are estimated up to 2021, fixing hyperparameters. Second, forecasts are generated recursively, producing one-step-ahead predictions for each country to almost one decade, from February of 2021 to July 2025⁸. This rolling design expands the training sample through time while generating strictly out-of-sample forecasts.

⁷Pseudo–real time means that at each forecast origin we restrict the information set to variables observable up to period t , thereby mimicking the information available to an agent standing at that point in time.

⁸This ensures that the ability of the models to predict the Russian-Ukraine invasion, the Israel-Hamas event and the Tariffs war by the US administration have been evaluated out-of-sample

Model accuracy is then evaluated by comparing forecasts with realized outcomes. Forecast errors from model m are defined under the rolling procedure as

$$e_{i,t+1}^{(m)} = y_{i,t+1} - \hat{y}_{i,t+1}^{(m)}, \quad (i, t) \in \mathcal{S}_{\text{roll}},$$

where $\mathcal{S}_{\text{roll}}$ denotes the set of out-of-sample forecast dates generated by the recursive rolling procedure. Accuracy is summarized by the mean absolute error (MAE) and root mean squared error (RMSE):

$$\text{MAE}^{(m)} = \frac{1}{|\mathcal{S}_{\text{roll}}|} \sum_{(i,t) \in \mathcal{S}_{\text{roll}}} |e_{i,t+1}^{(m)}|, \quad (3)$$

$$\text{RMSE}^{(m)} = \sqrt{\frac{1}{|\mathcal{S}_{\text{roll}}|} \sum_{(i,t) \in \mathcal{S}_{\text{roll}}} (e_{i,t+1}^{(m)})^2}, \quad (4)$$

where the square root in (4) highlights that RMSE is expressed in the same units as the dependent variable.

Given the unbalanced panel, we report results at multiple levels. At the **micro level**, metrics are computed pooling all country–day observations, i.e. using (3)–(4) over the entire set \mathcal{S} . At the **country level**, metrics are first computed separately for each country i and then averaged across countries and then balancing by the different data samples in some of the countries :

In sum, our design eliminates look-ahead bias, addresses the challenges of an unbalanced panel, and enables consistent comparison across model classes ranging from linear regressions to flexible machine learning methods. This methodological rigor provides a solid foundation for assessing how sentiment dynamics shape sovereign risk.

3.2 Do News Matter for Sovereign Risk? The Value of News-Based Indicators

By embedding news-based indicators into a recursive rolling forecasting framework alongside market benchmarks, we can evaluate both the incremental value of news and the types of models that extract the greatest predictive gains from their inclusion. This design allows us to ask whether linear regressions, tree-based ensembles, or neural networks benefit more from news relative to a market-only benchmark.

The benchmark specification includes only markets global financial variables: the two-year U.S. Treasury yield as a proxy for global interest rates (FED) and the VIX as a proxy for global financial volatility. These market benchmarks provide a clean baseline against which to evaluate the incremental power of news and reflect well-established external drivers of global financial assets and capital flows Calvo et al. (1993); Rey (2013); Miranda-Agricoppino and Rey (2020); Fratzscher (2012) among others

$$\mathbf{X}_{i,t}^{\text{Mkt}} = (\text{FED}_t, \text{VIX}_t).$$

The augmented specification enriches this baseline with high-frequency, more recently developed news-based indicators: the Geopolitical Risk Index (GPR), Economic Policy Uncertainty (EPU), Trade Policy Uncertainty (TPU), local economic sentiment (ECO), interest-rate sentiment (INT), and political tensions (POL):

$$\mathbf{X}_{i,t}^{\text{Mkt+News}} = (\mathbf{X}_{i,t}^{\text{Mkt}}, \text{GPR}_{i,t}, \text{EPU}_{i,t}, \text{TPU}_{i,t}, \text{ECO}_{i,t}, \text{INT}_{i,t}, \text{PolSent}_{i,t}).$$

For each model class m , one-step-ahead forecast errors are defined as:

$$e_{i,t+1}^{(m,k)} = y_{i,t+1} - \hat{y}_{i,t+1}^{(m,k)}, \quad k \in \{\text{Mkt}, \text{Mkt+News}\},$$

with predictive accuracy evaluated using mean absolute error (MAE) and root mean squared error (RMSE):

$$\text{MAE}^{(m,k)} = \frac{1}{|\mathcal{S}_{\text{roll}}|} \sum_{(i,t) \in \mathcal{S}_{\text{roll}}} |e_{i,t+1}^{(m,k)}|, \quad (5)$$

$$\text{RMSE}^{(m,k)} = \sqrt{\frac{1}{|\mathcal{S}_{\text{roll}}|} \sum_{(i,t) \in \mathcal{S}_{\text{roll}}} (e_{i,t+1}^{(m,k)})^2}. \quad (6)$$

The incremental predictive value of news is summarized by:

$$\Delta \text{MAE}^{(m)} = \text{MAE}^{(m, \text{Mkt})} - \text{MAE}^{(m, \text{Mkt+News})}, \quad (7)$$

$$\Delta \text{RMSE}^{(m)} = \text{RMSE}^{(m, \text{Mkt})} - \text{RMSE}^{(m, \text{Mkt+News})}. \quad (8)$$

Positive values of $\Delta \text{MAE}^{(m)}$ or $\Delta \text{RMSE}^{(m)}$ imply that news indicators enhance forecast accuracy relative to the market-only baseline. This framework thus isolates the marginal contribution of news while revealing which forecasting technologies—linear, nonlinear, or deep learning—are most effective in exploiting it.

By combining market variables with news-based indicators within a recursive rolling forecasting framework, we can jointly evaluate the incremental value of news and identify which model classes benefit most from their inclusion. This approach allows us to assess whether linear models, tree-based ensembles, or neural networks extract greater predictive gains from news relative to market-only benchmarks in a context of high frequency models.

Our benchmark specification includes only global financial variables, namely the two-year U.S. Treasury yield as a proxy for global interest rates (FED) and the a proxy for global financial volatility (VIX):

$$\mathbf{X}_{i,t}^{\text{Mkt}} = (\text{FED}_t, \text{VIX}_t).$$

The augmented specification enriches this baseline with high-frequency news-based indicators: the Geopolitical Risk Index (GPR), Economic Policy Uncertainty (EPU), Trade Policy Uncertainty (TPU), local economic sentiment (ECO), interest rate sentiment (INT), and political tensions (POL):

$$\mathbf{X}_{i,t}^{\text{Mkt+News}} = (\mathbf{X}_{i,t}^{\text{Mkt}}, \text{GPR}_{i,t}, \text{EPU}_{i,t}, \text{TPU}_{i,t}, \text{ECO}_{i,t}, \text{INT}_{i,t}, \text{PolSent}_{i,t}).$$

For each model class m , one-step-ahead forecast errors are defined as

$$e_{i,t+1}^{(m,k)} = y_{i,t+1} - \hat{y}_{i,t+1}^{(m,k)}, \quad k \in \{\text{Mkt}, \text{Mkt+News}\},$$

with forecast accuracy evaluated using mean absolute error (MAE) and root mean squared error (RMSE):

$$\text{MAE}^{(m,k)} = \frac{1}{|\mathcal{S}_{\text{roll}}|} \sum_{(i,t) \in \mathcal{S}_{\text{roll}}} |e_{i,t+1}^{(m,k)}|, \quad (9)$$

$$\text{RMSE}^{(m,k)} = \sqrt{\frac{1}{|\mathcal{S}_{\text{roll}}|} \sum_{(i,t) \in \mathcal{S}_{\text{roll}}} (e_{i,t+1}^{(m,k)})^2}. \quad (10)$$

The incremental predictive value of news-based variables is then measured by

$$\Delta \text{MAE}^{(m)} = \text{MAE}^{(m, \text{Mkt})} - \text{MAE}^{(m, \text{Mkt+News})}, \quad (11)$$

$$\Delta \text{RMSE}^{(m)} = \text{RMSE}^{(m, \text{Mkt})} - \text{RMSE}^{(m, \text{Mkt+News})}. \quad (12)$$

Positive values of $\Delta \text{MAE}^{(m)}$ or $\Delta \text{RMSE}^{(m)}$ indicate that news variables enhance predictive performance relative to the market-only benchmark. This exercise thus disentangles both the marginal role of news and the suitability of alternative forecasting technologies.

3.3 Model Interpretability with Shapley Values

We rely on out-of-sample performance to select the most appropriate model, since this criterion reflects the model's ability to learn patterns that generalize beyond the estimation sample and guards against overfitting. Once the best-performing specification is identified, we freeze its architecture and hyperparameters. We then apply it in-sample to trace the contribution of different drivers to sovereign risk over time, thereby using the model not for further prediction but as a disciplined lens to construct narratives of past episodes, in a predictive rather than structural sense.⁹ In the next step, we employ Shapley value decompositions to open the model's “black box” and attribute risk dynamics to their underlying drivers.

⁹The Shapley analysis is interpretive rather than causal: it attributes model-implied variation in sovereign risk to input variables, reflecting predictive importance rather than structural identification.

Having fixed the preferred specification, we turn to interpretability. Specifically, we use Shapley values to decompose contemporaneous sovereign CDS spreads into contributions from global, macroeconomic, and political-geoeconomic sentiment factors. This allows us to reconstruct the role of each driver throughout the sample and to build narratives around key historical episodes. Therefore, for interpretability purposes, we apply the same specification for sovereign risk contemporaneously

$$y_{i,t} = f^*(X_{i,t}) + \varepsilon_{i,t},$$

where $y_{i,t}$ is the CDS spread for country i , $X_{i,t}$ stacks global, macro, and political/geoeconomic sentiment inputs (and their lags), and f^* is the best-performing machine-learning model selected on the basis of the out-of-sample horse race exercise. To *understand the past*, we freeze f^* and compute Shapley values for every historical observation, obtaining factor- and country-specific attributions $\{\phi_{j,i,t}\}$ that exactly decompose the model-implied component of the spread:

$$\hat{y}_{i,t} \equiv f^*(X_{i,t}) = \phi_0 + \sum_{j=1}^M \phi_{j,i,t},$$

with the residual $\varepsilon_{i,t} = y_{i,t} - \hat{y}_{i,t}$ capturing idiosyncratic variation. This setup lets us trace, *ex post*, how much of each day's realized spread is attributed by the model to each driver and how those attributions evolve across time and countries.

In this paper, Shapley values are employed to decompose movements in sovereign CDS spreads into contributions from global, macroeconomic, and political/geoeconomic sentiment factors. These attributions are model-based and predictive rather than causal: they reflect how the machine-learning models map inputs into risk predictions, without requiring strong exogeneity assumptions.

Once the most robust model has been identified out-of-sample through the horse race competition, we turn to an in-sample analysis of the determinants of past CDS spreads. While non-linear machine-learning models are well suited to capturing complex patterns, their internal structure often functions as a “black box,” making it difficult to interpret how predictions are generated (Mullainathan and Spiess, 2017)¹⁰. To address this challenge, we employ the Shapley Values (Lundberg and Lee, 2017), an algorithm inspired by the theory of cooperative games which provide a rigorous, game-theoretic framework (Shapley, 1953) for attributing model predictions to individual input variables.

The Shapley framework offers properties that distinguish it from other interpretability methods. It is the only attribution approach that is both *locally accurate* and *consistent*. Local accuracy ensures that the sum of feature attributions exactly equals the model's prediction for each observation, while consistency guarantees that if a feature's impact on predictions increases in the model, its attribution cannot decrease. These properties, together with linearity, symmetry, and the exclusion of noise features, make SHAP uniquely robust for interpreting complex, non-linear models (Molnar, 2019)¹¹.

Formally, SHAP attributes a model prediction $f(x)$ for a given instance x to its input features $\phi_j(x)$ according to the additivity property:

$$f(x) = \phi_0 + \sum_{j=1}^M \phi_j(x), \quad (13)$$

where M is the number of features, ϕ_0 is the baseline (average) prediction, and $\phi_j(x)$ represents the marginal contribution of feature j . This additive decomposition ensures that each prediction can be fully explained by the contributions of its inputs. An additional advantage of this framework is that it can be applied to every observation in the time series, allowing us to decompose the explanatory factors of risk dynamically. In this way, we can trace how the relevance of specific drivers (e.g., Geopolitical Risk, VIX, or monetary policy) evolves over time, capturing periods when particular variables gain or lose importance in shaping sovereign CDS spreads.

I

Beyond main effects, we use SHAP *interaction values* to quantify pairwise complementarities and threshold behavior. The attribution for feature j can be decomposed as

$$\phi_j(x) = \sum_{i=1}^M \phi_{ij}(x) = \phi_{jj}(x) + \sum_{i \neq j} \phi_{ij}(x), \quad (14)$$

where $\phi_{jj}(x)$ is the main (own) effect and $\phi_{ij}(x)$ captures the joint effect of features i and j (e.g., how the influence of Geopolitical Risk depends on the level of VIX). Additionally, in the next section we explain how we can document interaction-driven threshold effects and to attribute “spillovers” *across variables* within the model.

¹⁰We implement the shapley values using the open source python code SHAP which can be downloadable here <https://shap.readthedocs.io/en/latest/>

¹¹Alternative methods such as LIME (Ribeiro et al., 2016) or DeepLIFT do not satisfy these criteria (Lundberg and Lee, 2017).

3.4 Sovereign risk Spill-Overs and Interconnectedness

To enhance our analysis, we employ two complementary measures of interconnectedness applied to the panel of daily, country-level Shapley values generated by the machine learning model. The first tool, the *Diebold–Yilmaz Spillover Index (DY)*, captures directional and dynamic propagation of shocks through a parametric VAR-based framework (Diebold and Yilmaz, 2012b). The second, a *Network Density Measure* (Newman, 2010), provides a nonparametric view of contemporaneous synchronization across countries, drawing on the financial networks literature (e.g., Battiston et al., 2016; Barabási, 2016; Alter and Beyer, 2014). Taken together, the two indices are natural complements: DY highlights dynamic, directional spillovers, while density isolates contemporaneous co-movement without imposing parametric structure.¹²

The DY spillover index quantifies the extent to which forecast error variance in one country's Shapley values is explained by shocks originating in other countries. We estimate a Vector Autoregression (VAR) model for the rolling panel of Shapley values and compute the Generalized Forecast Error Variance Decomposition (GFEVD). The resulting spillover matrix $\Theta(H)$ summarizes how much each country contributes to the variance of others at horizon H . The DY index is then defined as the normalized sum of the off-diagonal elements of $\Theta(H)$:

$$S(H) = \frac{1}{N} \sum_{\substack{i,j=1 \\ i \neq j}}^N \tilde{\theta}_{ij}(H) \times 100 \quad (15)$$

where $\tilde{\theta}_{ij}(H)$ denotes the normalized contribution of country j to the forecast error variance of country i . High values of $S(H)$ indicate stronger cross-country transmission of shocks in the Shapley values attribution space.

As a robust and complementary perspective, we compute a *Weighted Network Density* statistic that captures the intensity of contemporaneous comovement, independent of parametric dynamics. Specifically, we calculate pairwise Spearman rank correlations of Shapley values across countries and retain links whose absolute correlation exceeds a threshold τ . Formally, the weighted density is defined as:

$$D_w(\tau) = \frac{\sum_{i=1}^{N-1} \sum_{j=i+1}^N |\rho_{ij}| \cdot \mathbf{1}_{|\rho_{ij}| \geq \tau}}{\frac{N(N-1)}{2}} \quad (16)$$

where $|\rho_{ij}|$ is the absolute correlation between countries i and j , and $\mathbf{1}_{|\rho_{ij}| \geq \tau}$ indicates whether the link exceeds the threshold. This measure is *model-light* and nonparametric: it requires no assumptions about lags or forecast horizons and is robust even in short rolling samples where VAR estimates can be unstable.

Taken together, these indices capture distinct aspects of interconnectedness. DY measures *directional spillovers*, while density reflects *synchronous co-movement*. Episodes of high density but low DY suggest common shocks or global news bursts without clear propagation channels; high DY with modest density points to contagion concentrated in specific links; simultaneous increases in both correspond to periods of systemic stress. This dual-metric framework thus provides a richer and more policy-relevant picture of cross-country risk linkages.

4 Machine Learning and Shapley values Empirical Results

4.1 Out of Sample Overall Model Performance

The empirical horse race compares alternative model classes based on their out-of-sample predictive accuracy. As outlined in the theoretical section, models are evaluated using a recursive forecasting framework with appropriate train–test separation to avoid look-ahead bias and leakage around moving-average windows.

Out-of-sample forecast errors are assessed through standard loss functions, namely mean absolute error (MAE) and root mean squared error (RMSE). Given the presence of strong nonlinearities and marked cross-country heterogeneity, MAEs are relatively high in absolute terms.

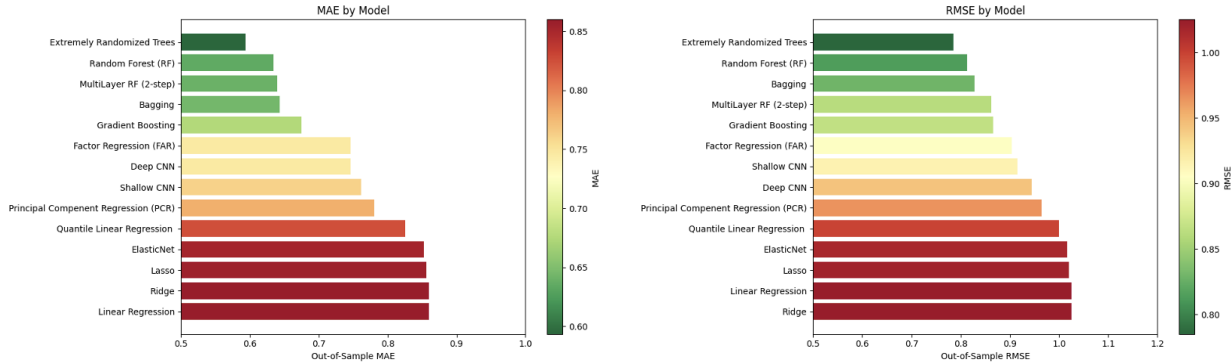
¹²This contrast is crucial for interpretation. Episodes of high density but low DY suggest common shocks that trigger simultaneous responses without clear propagation channels. High DY with modest density points to contagion concentrated in specific bilateral links. Simultaneous increases in both correspond to periods of systemic stress, where shocks both synchronize markets and transmit directionally across borders. The dual-metric framework therefore yields a richer and more policy-relevant picture of cross-country risk linkages than any single approach alone. We apply both measures in Section 4 to trace how sovereign risk interconnectedness evolved during major geopolitical and financial episodes

Figure 2 summarizes the pseudo real-time out-of-sample performance across all model classes, ranked by MAE and RMSE. Four distinct tiers emerge:

- *Ensemble Tree methods (Random Forest family) dominate.* ($MAE \lesssim 0.60$, $RMSE \lesssim 0.80$). Extremely Randomized Trees deliver the lowest forecast errors, followed closely by Random Forests, the two-step Multilayer Random Forest, and Bagging. Gradient Boosting also performs strongly (Friedman, 2001). These flexible non-linear ensembles excel because they accommodate interactions, threshold effects, and higher-order dependencies.
- *Convolutional Neural Networks (CNNs) reach intermediate accuracy.* ($MAE \approx 0.70$ – 0.80 , $RMSE \approx 0.85$ – 0.90). Both shallow and deeper CNN architectures outperform linear baselines, indicating that automatic feature extraction can capture useful nonlinear patterns. However, their gains are not sufficient to consistently match the robustness of tree ensembles (LeCun et al., 2015).
- *Linear reduction methods achieve modest improvements.* ($MAE \approx 0.70$ – 0.80 , $RMSE \approx 0.85$ – 0.95). Factor-Augmented Regressions and Principal Component Regression perform somewhat better than pure linear models but below CNNs and ensembles. While dimension reduction helps mitigate noise and collinearity, it cannot fully capture nonlinear dynamics (Stock and Watson, 2002; Jolliffe, 2002).
- *Linear benchmarks underperform.* ($MAE \gtrsim 0.80$, $RMSE \gtrsim 0.95$). Standard OLS, regularized regressions (Ridge, Lasso, Elastic Net), and Quantile Regression exhibit the highest forecast errors. Regularization reduces variance but cannot correct the bias from linear misspecification (Hastie et al., 2009). Quantile regression provides an alternative by targeting conditional distributional tails, but it still relies on a linear functional form, which limits its ability to capture the nonlinear dynamics present in sovereign risk spreads (Koenker and Bassett, 1978).

The results reveal that nonlinear ensemble methods provide the lowest out-of-sample MAE and RMSE, consistent with the view that financial and economic prediction problems are characterized by strong interactions, state dependence, and threshold effects (Varian, 2014; Mullainathan and Spiess, 2017; Gu et al., 2020). Tree-based ensembles work well because they automatically partition the data in a flexible way, enabling them to handle very different types of predictors (Breiman, 2001; Goulet Coulombe et al., 2022). Similar findings appear in studies that use financial variables as early-warning predictors of crises (Bluwstein et al., 2023). By contrast, convolutional neural networks do not dominate

Figure 2: Comparison of Overall Model Performance (Out-of-Sample MAE & RMSE)



Notes: These figures compare the out-of-sample forecasting performance of alternative models using mean absolute error (MAE, left panel) and root mean squared error (RMSE, right panel). Ensemble-based approaches—Extremely Randomized Trees, Random Forests, Multilayer Random Forests (2-step), and Bagging—consistently achieve the lowest prediction errors. Gradient boosting and factor-augmented regression (FAR) also perform competitively, followed by convolutional neural networks (Shallow CNN and Deep CNN) and principal component regression (PCR). Traditional linear estimators—Ordinary Least Squares, Ridge, Lasso, ElasticNet, and Quantile Regression—systematically underperform, underscoring the importance of nonlinear and ensemble methods in capturing complex predictive structures.

here. With smoothed, short-lag predictors, their advantage in extracting spatial or temporal structure is limited in our setting. This outcome aligns with benchmarks showing that tree ensembles often outperform deep networks on tabular economic data.

Linear methods consistently appear at the bottom of the rankings. While shrinkage and dimensionality reduction help control variance, they cannot address the systematic bias that arises when the true data-generating process is nonlinear.

In sum, ensemble-based methods—especially the Random Forest family—emerge as the most reliable performers in modeling sovereign-risk dynamics shaped by global volatility, sentiment, and geopolitical shocks. Neural networks may yield further gains with architectures tailored to long-horizon dependencies (e.g., temporal convolutional networks or transformers). Linear models remain the least effective.

4.2 Value of News-Based Predictors

We next evaluate whether news-based indicators add predictive power beyond standard market benchmarks. The comparison contrasts two information sets: a *Markets-Only* benchmark, which relies on the 2-year yield (a proxy for global monetary policy) and the VIX (global volatility), and an *extended specification* that augments these market indicators with text-based measures of geopolitical risk, policy and trade uncertainty, and macroeconomic sentiment (hereafter *Markets+News*). Forecast accuracy is assessed using out-of-sample RMSE and MAE across a broad range of estimators, including linear regressions, dimensionality-reduction approaches, tree-based ensembles, and shallow and deep neural networks. Three main findings emerge from Table 1.

- *Systematic gains for Markets+News across models.* All 14 models perform better when news variables are included. Even linear specifications register RMSE reductions of 5–6 percent, underscoring that text-based indicators provide incremental information not contained in standard financial predictors.
- *Larger improvements in nonlinear models.* The most pronounced gains arise in tree-based ensembles. Bagging reduces RMSE by 15.7 percent, while the Multilayer Random Forest achieves a 24 percent reduction. These results indicate that the predictive content of news is not simply linear sentiment but operates through complex, nonlinear interactions that require flexible methods to be fully exploited.
- *Tree ensembles dominate.* Across specifications, ensembles consistently deliver the largest improvements, highlighting their ability to capture intricate interactions and handle the noisy, high-dimensional structure of text data.

Table 1: Forecast Accuracy: Markets-Only vs. Markets+News

Machine Learning Model	News Extended Models		Markets Only Model		Difference NEWS vs Benchmark Model			
	Market Variables + News Variables		Market Variables (2Y Yields + VIX)		RMS		MAE	
	RMSE	MAE	RMSE	MAE	Diff	% Var	Diff	% Var
Linear Regression	1.0253	0.8601	1.0876	0.9192	-0.06	-5.7%	-0.06	-6.4%
Lasso	1.0203	0.8562	1.0829	0.9156	-0.06	-5.8%	-0.06	-6.5%
Ridge	1.0253	0.8600	1.0875	0.9191	-0.06	-5.7%	-0.06	-6.4%
Elastic Net	1.0165	0.8526	1.0793	0.9119	-0.06	-5.8%	-0.06	-6.5%
Quantile Linear Regression	0.9993	0.8521	1.0614	0.8826	-0.06	-5.9%	-0.03	-3.5%
Principal Components (PCR)	0.9643	0.7807	0.9372	0.7335	0.03	2.9%	0.05	6.4%
Factor Models (FAR)	0.9038	0.7457	0.8947	0.7195	0.01	1.0%	0.03	3.6%
Gradient Boosting	0.8661	0.6752	0.9835	0.7900	-0.12	-11.9%	-0.11	-14.5%
Bagging	0.8281	0.6436	0.9818	0.7661	-0.15	-15.7%	-0.12	-16.0%
Random Forest	0.8135	0.6345	1.0257	0.7589	-0.21	-20.7%	-0.12	-16.4%
Extremely Randomized Trees	0.7849	0.5933	1.0036	0.7318	-0.22	-21.8%	-0.14	-18.9%
Multilayer Random Forest (2S)	0.8617	0.6434	1.1047	0.8192	-0.24	-22.0%	-0.18	-21.5%
Shallow CNN	0.9157	0.7613	1.0316	0.8633	-0.12	-11.2%	-0.10	-11.8%
Deep CNN	0.9440	0.7458	1.0373	0.7837	-0.09	-9.0%	-0.04	-4.8%

Notes: The table reports out-of-sample RMSE and MAE for models estimated with and without news-based predictors. The right panel reports percentage differences relative to the Markets-Only benchmark.

These results imply that news-based indicators capture aspects of sovereign risk not fully priced in by contemporaneous financial variables (Baker et al., 2016; Caldara and Iacoviello, 2022). The performance gains are nonlinear: improvements scale with the model’s ability to accommodate high-order interactions. This pattern resonates with the growing evidence that unstructured, high-frequency data contain predictive signals beyond traditional fundamentals (Gentzkow et al., 2019; Manela and Moreira, 2017; Davis et al., 2025).

More broadly, the findings highlight that the forecasting value of news depends not only on their inclusion but also on the way they are incorporated into the model. Linear specifications deliver modest improvements, while nonlinear approaches yield markedly stronger gains, consistent with arguments that economic prediction problems involve interactions, state dependence, and threshold effects (Varian, 2014; Mullainathan and Spiess, 2017; Athey and Imbens, 2019). This underscores that both the choice of predictors and the choice of method are crucial when integrating text-based indicators into macro-financial forecasting frameworks.

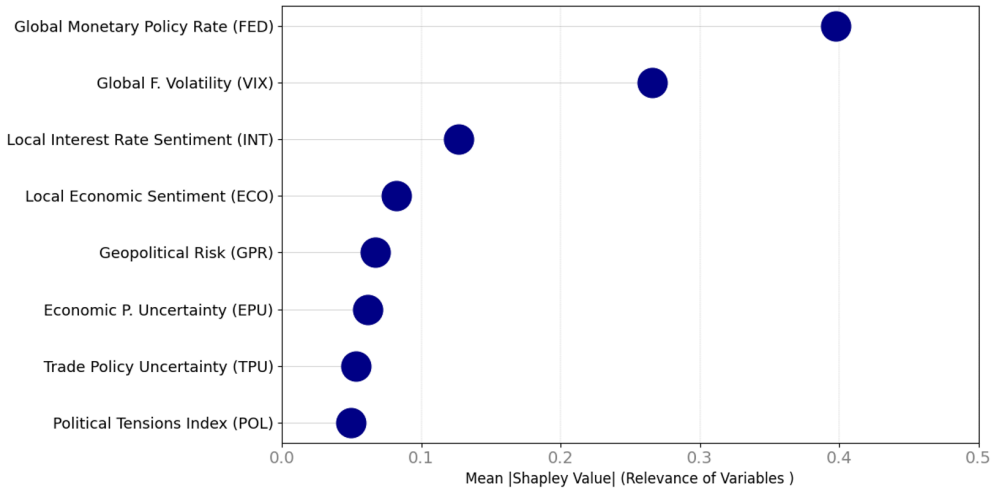
4.3 The Determinants of Sovereign Risk through Shapley Values

4.4 Determinants of Sovereign Risk: SHAP Evidence

The analysis of feature importance from the Multilayer Random Forest, summarized in the mean absolute SHAP value plot in Figure 3, reveals a clear hierarchy in the drivers of sovereign risk.

Global “push” variables dominate. The *Global Monetary Policy Rate* (proxied by the 2-year U.S. Treasury yield) and *Global Financial Volatility* (VIX) emerge as the most influential predictors. This finding aligns with the literature on the global financial cycle, emphasizing the central role of U.S. monetary policy in shaping global risk appetite and capital flows to both emerging and advanced economies (Rey, 2013; Miranda-Agricocco and Rey, 2020). The prominence of the VIX further corroborates its role as a barometer of global risk aversion, with spikes in volatility often preceding capital flow reversals and widening sovereign spreads (Gelos et al., 2011).

Figure 3: Variable Importance in Sovereign Risk Models (Shapley Values, 2018–2025)



Notes: The figure reports mean absolute Shapley values, which quantify the contribution of each predictor to sovereign CDS spreads (2018–2025). Global monetary policy (2-year UST) and global financial volatility (VIX) dominate, followed by domestic interest rate and economic sentiment. Geopolitical risk, economic and trade policy uncertainty, and political tensions also contribute, though to a lesser extent.

Beyond these global forces, domestic “pull” factors—particularly *Local Interest Rate Sentiment* and *Local Economic Sentiment*—rank next in importance. This highlights that while global conditions set the baseline, country-specific fundamentals and their perception by investors remain critical in differentiating sovereign risk (Eichengreen et al., 2021).

Among non-economic factors, the *Geopolitical Risk Index (GPR)* stands out, consistent with evidence that geopolitical tensions raise sovereign borrowing costs by depressing growth expectations and investor confidence (Caldara and Iacoviello, 2022). The *Economic Policy Uncertainty (EPU)* and *Trade Policy Uncertainty (TPU)* indices also register meaningful contributions, in line with research showing that uncertainty over future policies deters investment and elevates credit risk (Baker et al., 2016). Finally, the *Political Tensions Index (POL)*, though the least influential, still matters, confirming that political instability is a priced component in sovereign debt markets. Taken together, these non-economic variables are influential but clearly less central than global monetary and financial drivers or domestic macroeconomic sentiment, underscoring their role as secondary amplifiers rather than primary determinants of sovereign risk.

4.5 Asset Class and Cross-Country Heterogeneity in Sovereign Risk Drivers

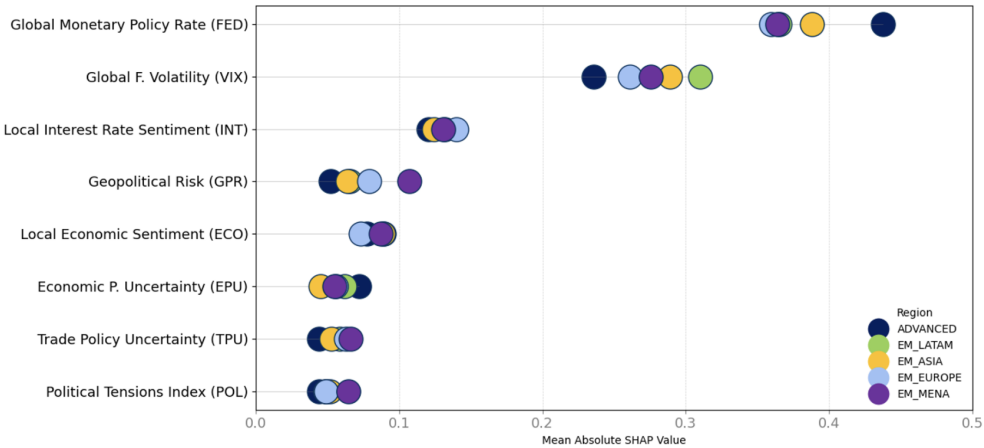
The disaggregated SHAP analysis in Figure 4 reveals substantial heterogeneity in the determinants of sovereign risk across advanced and emerging markets, as well as across EM regions.

A first result is the universal importance of global drivers. Both advanced and emerging market (EM) sovereign assets are highly sensitive to shifts in global monetary policy and global financial volatility, confirming the pervasive reach of the global financial cycle (Rey, 2013; Miranda-Agrippino and Rey, 2020). Yet important differences emerge. Advanced economies are more exposed to the *global policy rate* (2-year U.S. Treasury yield), consistent with their tighter integration into global yield curves. By contrast, EMs are more reactive to *global financial volatility* (VIX), reflecting the “risk-on/risk-off” paradigm in which capital flows to EMs respond disproportionately to swings in risk appetite (International Monetary Fund, 2019). This pattern is especially pronounced in Latin America and, to a lesser extent, Emerging Asia, where the VIX dominates as a risk factor.

Domestic “pull” factors provide an additional layer of differentiation. Local economic and interest rate sentiment contribute more to sovereign risk pricing in EMs than in advanced economies, underscoring the role of domestic fundamentals once global conditions are controlled for (Eichengreen et al., 2021).

Non-economic risks show sharper regional asymmetries. Geopolitical risk (GPR) has moderate effects overall but emerges as a leading determinant in the Middle East, where geopolitical tensions are endemic (Caldara and Iacoviello, 2022). Similarly, Economic Policy Uncertainty (EPU) contributes more in advanced economies than in EMs, suggesting that policy ambiguity is already priced into EM assets, whereas deviations from stability norms carry greater weight in advanced markets (Baker et al., 2016).

Figure 4: Sovereign Risk determinants by asset class and regions (Shapley Values 2018-2025)

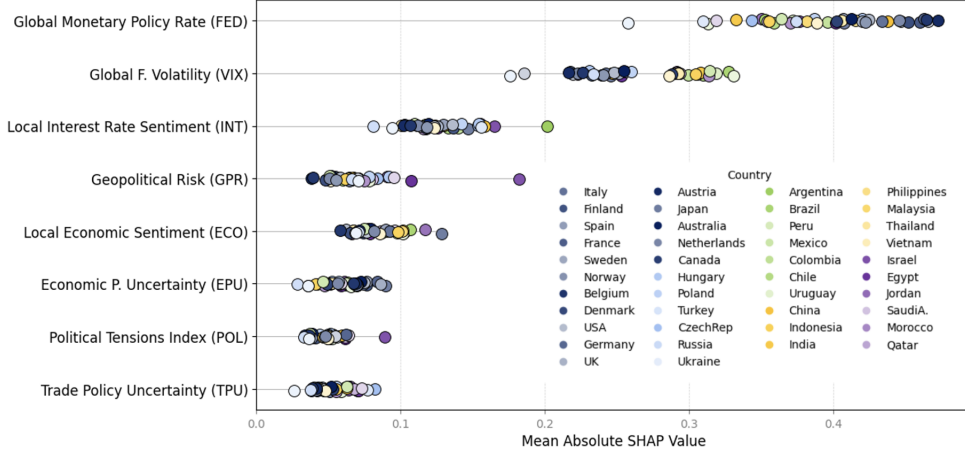


Notes: This Figure reports mean absolute SHAP values by region and asset class, highlighting the relative importance of predictors for sovereign CDS spreads. Global monetary policy rates (2-year UST) and global financial volatility (VIX) dominate across all regions, though the magnitude of their influence varies. Local factors—especially interest rate sentiment and economic sentiment—contribute more in emerging markets (Latin America, Asia, Europe, and MENA) than in advanced economies. By contrast, uncertainty measures (Geopolitical Risk, Economic Policy Uncertainty, and Trade Policy Uncertainty) play a secondary role, and political tensions have the weakest explanatory power. The findings suggest that while global drivers are primary determinants, local sentiment indicators provide additional explanatory content in emerging markets.

The country-level decomposition in Figure 5 further illustrates these dynamics. Brazil, Mexico, and the Philippines stand out as particularly exposed to shifts in global risk appetite, consistent with their large weights in EM bond indices such as the JP Morgan EMBI. By contrast, China appears comparatively insulated, reflecting its financial segmentation. Geopolitical risk is generally minor but becomes the dominant driver for countries at the center of conflict, such as Ukraine, Israel, and Russia, with measurable spillovers to neighbors including Poland and Finland. Economic Policy Uncertainty (EPU) is slightly more relevant in advanced economies, particularly the United States, Germany, France, and the UK, reinforcing the notion that unexpected policy shifts in traditionally stable jurisdictions are more heavily priced by investors.

Taken together, these findings confirm the primacy of global financial conditions while showing that regional and country-specific sensitivities generate systematic heterogeneity. Sovereign risk pricing is shaped not only by the global cycle but also by local fundamentals and political shocks, with Shapley value analysis highlighting where global patterns dominate and where idiosyncratic deviations matter most.

Figure 5: Sovereign Risk determinants by Country (Shapley Values 2018-2025)

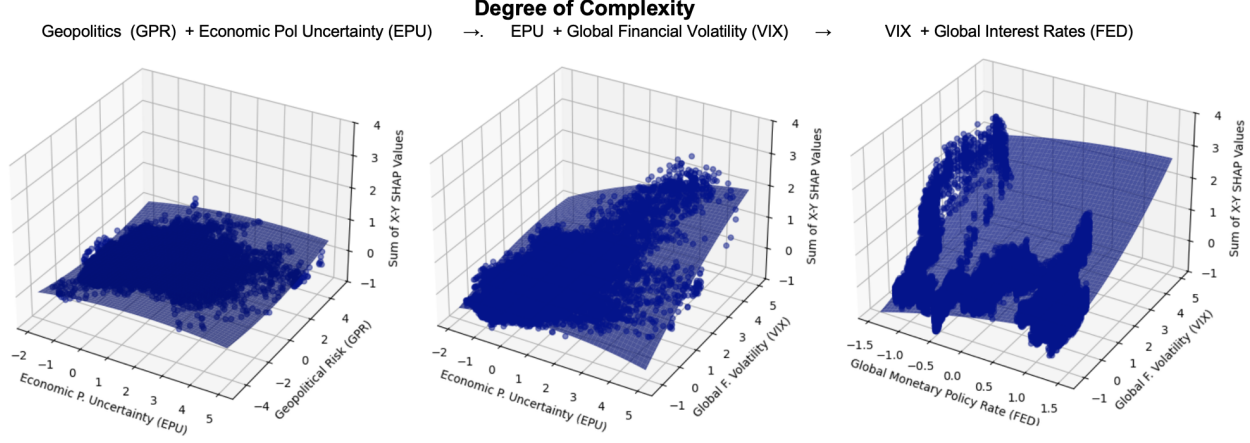


Notes: The Figure displays mean absolute SHAP values by country, decomposing the relative contribution of global, local, and uncertainty variables to sovereign CDS spreads. Global drivers—particularly the 2-year U.S. Treasury rate and global financial volatility (VIX)—dominate across most countries, though their relative importance varies. Local interest rate and economic sentiment indicators play a more prominent role in emerging markets, while advanced economies exhibit greater reliance on global factors. Uncertainty measures (Geopolitical Risk, Economic Policy Uncertainty, and Trade Policy Uncertainty) show heterogeneous contributions, with higher relevance in politically volatile or trade-dependent economies. Political tensions remain the weakest determinant across the country sample.

4.6 Geopolitics, Economic uncertainty and Global Markets

Leveraging the additive property of Shapley values Lundberg and Lee (2017), we construct three two-factor scenarios that capture escalating layers of complexity in sovereign risk determination: from localized political and policy uncertainty to global financial tightening. Figures 6–7 display the Shapley dependence plots for developed and emerging economies, respectively.

Figure 6: Shap Contribution by Variables in Developed Economies: Shap Dependence Plots



Notes: The figure illustrates the combined impact of key predictors on sovereign CDS spreads for the Developed Markets, using SHAP dependence plots. The bottom row displays the combined influence of geopolitical risk and economic policy uncertainty for Developed Economies. The middle row plots the joint contribution of economic policy uncertainty (EPU) and global volatility (VIX). The top row shows the joint effect of global financial volatility (VIX) and global monetary policy (FED), highlighting strong nonlinear interactions across both advanced and emerging markets. These results underscore the layered nature of risk transmission, with global shocks interacting with local vulnerabilities to shape sovereign risk outcomes.

- *Scenario 1: Geoeconomics and Policy Uncertainty.* This baseline scenario assesses the combined impact of Geopolitical Risk (GPR) and Economic Policy Uncertainty (EPU). It isolates the effects of non-financial uncertainty, representing the foundational layer of risk stemming from the political and policy-making environment (Baker et al., 2016; Caldara and Iacoviello, 2022).
- *Scenario 2: Uncertainty and Financial Volatility.* This second scenario models an escalation where policy uncertainty spills over into financial markets. It evaluates the interaction between Economic Policy Uncertainty (EPU) and Global Financial Volatility (VIX), capturing how market sentiment amplifies the risks associated with an unpredictable policy landscape.
- *Scenario 3: Global Financial Conditions.* The third and most acute scenario represents a comprehensive tightening of global financial conditions. It combines Global Financial Volatility (VIX) with shifts in Global Monetary Policy, illustrating the potent impact of a simultaneous risk-off shock and a rise in global funding costs, core tenets of the Global Financial Cycle literature.

The scenario analysis described in the graphs of Figure 6 reveals significant non-linearities and interactions. *The first scenario shows the relatively weaker impact of isolated Geopolitical and Economic uncertainty combination.* The combined influence of geopolitical risk and economic policy uncertainty on sovereign CDS spreads is, for most regions, marginal. The relatively flat surfaces in the plots indicate a low sensitivity to these factors in isolation. However, regional heterogeneity is apparent. The Middle East influenced by structural instability and, to a lesser extent, Emerging Europe influenced by the Russian invasion to Ukraine display a more pronounced upward slope, confirming that sovereign risk in these geopolitically sensitive regions is more vulnerable to flare-ups in political and policy-related tensions.

The second scenario shows the amplification of economic policy uncertainty through Financial Volatility. The picture changes dramatically in Scenario 2, which underscores the role of financial markets as an amplifier of risk. When economic policy uncertainty is combined with a rise in global volatility (VIX), the impact on sovereign risk is significantly elevated. This aligns with theories of uncertainty shocks, which posit that their effects are magnified under conditions of financial stress (Bloom, 2009). The steeper planes in the plots illustrate a powerful positive interaction: high economic policy uncertainty in a high-VIX environment is substantially more detrimental than either shock occurring alone.

The latest scenario reveals the critical role of Monetary Policy and Financial condition. This constitutes the most powerful risk combination. A simultaneous spike in global volatility and a tightening of global monetary policy leads to a sharp and non-linear increase in sovereign risk. This captures the essence of the global financial cycle, where U.S. monetary policy and global risk aversion act as dominant “push” factors for international capital flows and risk premia.

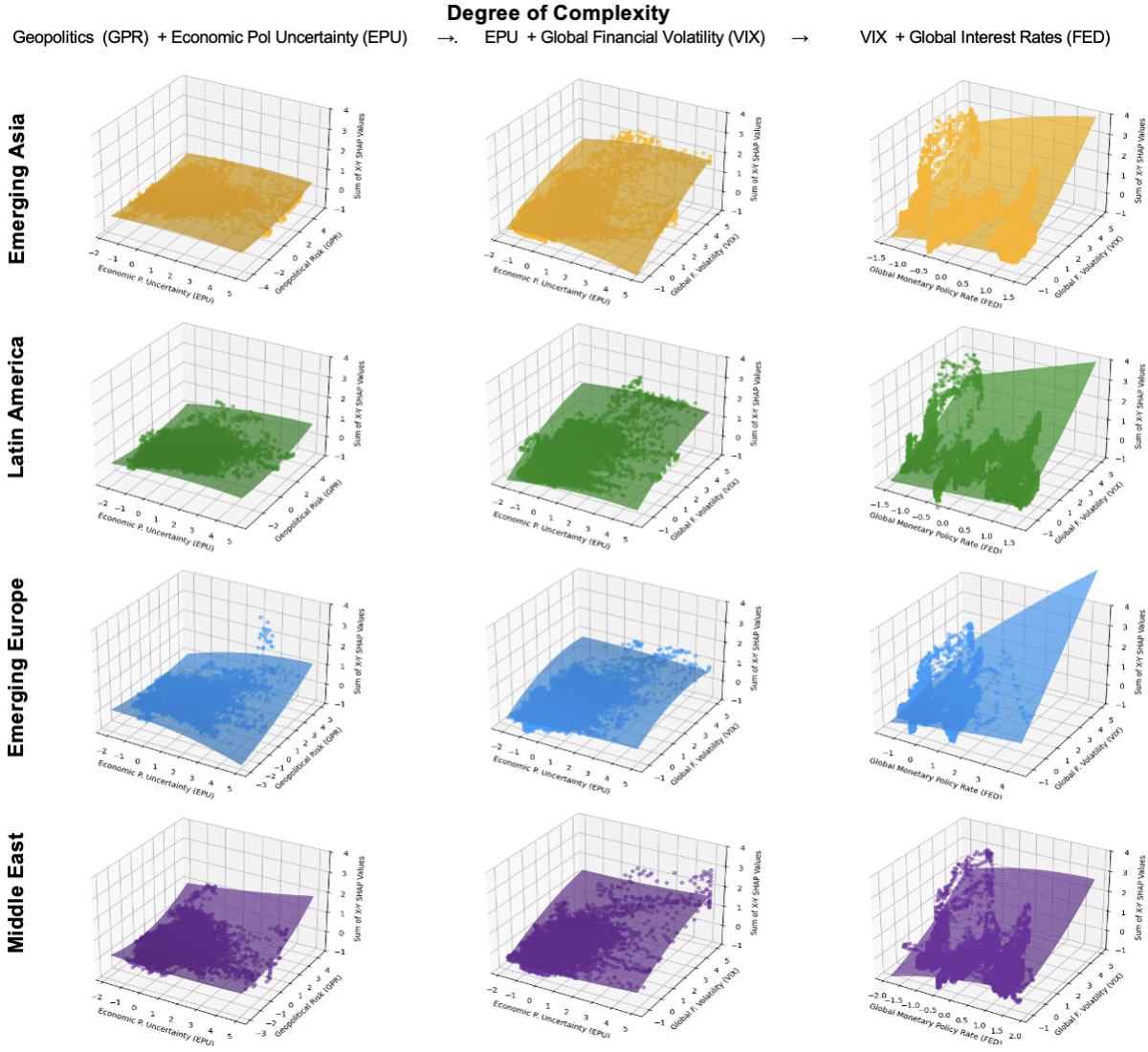
Additionally, the scenario shows that the impact of a sharp increase in global volatility can be partially contained when interest rates remain low. However, this mitigating effect is weaker than the potent amplification that occurs when both factors rise in tandem. The impact of a volatility shock is markedly non-linear and state-dependent (Bekaert et al., 2013); it is powerfully amplified when monetary policy is tight (Rey, 2013; Miranda-Agrippino and Rey, 2020) and partially contained when policy is accommodative, for instance, through the risk-taking channel (Bruno and Shin, 2015), (Miranda-Agrippino and Rey, 2020). The steep, often convex, surfaces in the plots show that as financial conditions tighten, the sensitivity of sovereign spreads accelerates. The implication is clear: if an uncertainty shock triggers not only a rise in the VIX but also a hawkish monetary policy response, the repercussions for sovereign risk are severe.

In summary, the scenarios reveal a critical transmission channel. *Geoeconomic or policy uncertainty, while often manageable in isolation, becomes a potent threat when it contaminates global financial volatility and tightens financial conditions.* The complexity and interaction between these domains are paramount in determining sovereign vulnerability.

4.7 Interconnectedness and Network Density Results

Figure 8 summarizes dynamic networks in the *Shapley attribution space* using the two complementary indices introduced above: the Diebold–Yilmaz (DY) total spillover index (blue line) and the weighted network density (orange line). Panels track connectedness across countries for each variable group from 2021 onward, with vertical markers for the Russia–Ukraine invasion (Feb 2022), the Hamas–Israel conflict (Oct 2023), and the 2024 U.S. election. Read jointly, DY captures dynamic directional spillovers while density reflects synchronous co-movement. The joint patterns distinguish between system-wide stress, common but transient shocks, and directional propagation through specific channels. Three main patterns emerge:

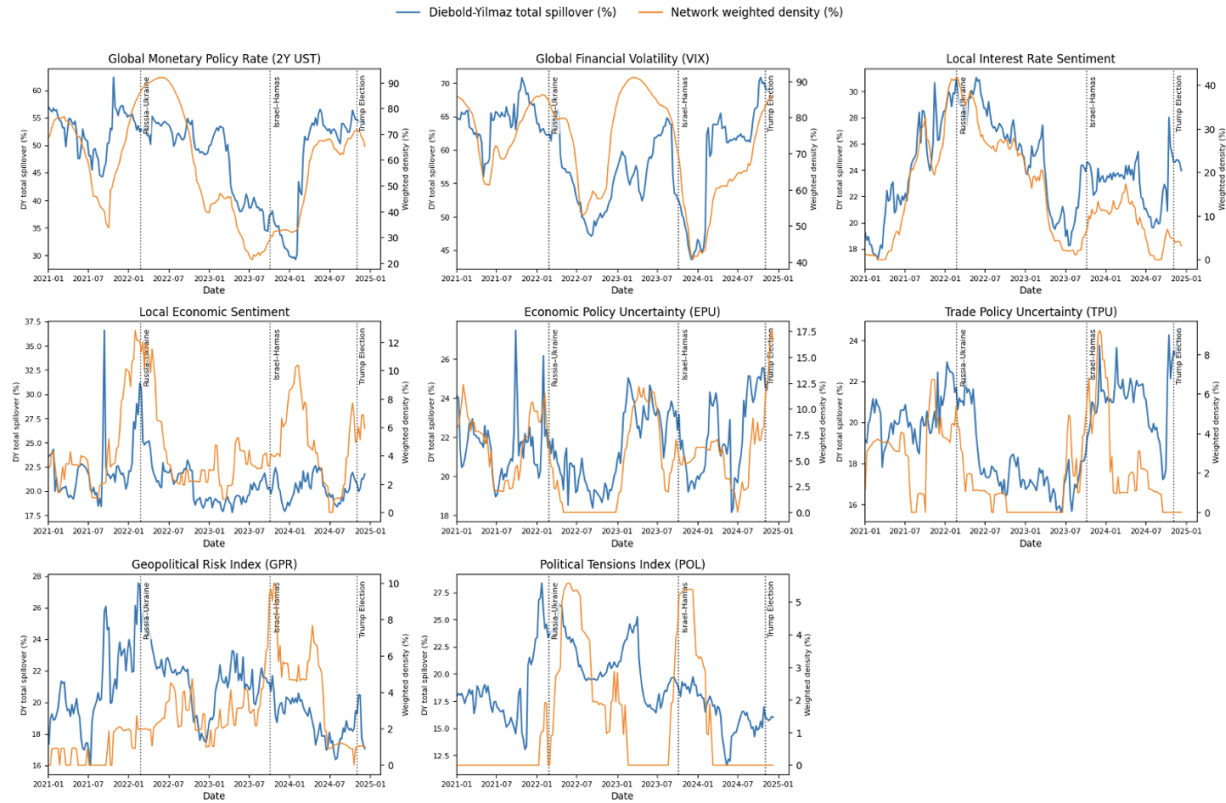
Figure 7: Shap Contribution by Variables in Emerging Regions: Shap Dependence Plots



Notes: The figure illustrates the combined impact of key predictors on sovereign CDS spreads across Emerging Market Regions, using Shapley dependence plots. The bottom row displays the combined influence of geopolitical risk and economic policy uncertainty. The middle row plots the joint contribution of economic policy uncertainty (EPU) and global volatility (VIX). The top row shows the joint effect of global financial volatility (VIX) and global monetary policy (2-year UST), highlighting strong nonlinear interactions across both advanced and emerging markets. Across all cases, global drivers dominate, but their interaction with domestic uncertainty amplifies sovereign risk particularly in emerging regions (Latin America, Asia, Europe, and MENA). These results underscore the layered nature of risk transmission, with global shocks interacting with local vulnerabilities to shape sovereign risk outcomes.

- *Global financial conditions are the dominant and persistent transmitters.* The global monetary policy rate (2-year UST) and global financial volatility (VIX) exhibit the highest and most sustained DY values. Both spike sharply in early 2022, normalize through mid-2023, and re-accelerate into late 2024. Density moves in tandem with DY, consistent with system-wide repricing rather than localized contagion. This confirms that cross-country propagation of sovereign risk is primarily mediated by global rates and volatility.
- *Local macro sentiment transmits directionally but with limited persistence.* Local interest rate sentiment shows large DY increases during 2022, coincident with the global tightening–volatility shock, but density collapses thereafter even as DY remains non-negligible. This pattern—moderate DY with low density—signals directional propagation through monetary channels without sustained synchronization. Local economic

Figure 8: Diebold–Yilmaz Spillovers and Network Density (2021–2025)



Notes: The figure reports dynamic spillover effects (blue line) and network density (orange line) for sovereign risk determinants. Top row: global financial drivers (2-year UST, VIX, local interest rate sentiment); middle row: local economic sentiment and uncertainty indices (EPU, TPU); bottom row: geopolitical risk (GPR) and political tensions (POL).

sentiment contributes more gradually: DY trends upward into 2024–2025, but density remains sporadic, indicating slow diffusion rather than burst-like contagion.

- *Geopolitical and policy uncertainty shocks are episodic and synchronous.* Geopolitical risk (GPR) and political tensions (POL) show sharp density spikes around October 2023, during the Hamas–Israel conflict, but DY remains muted—an archetypical “common news” episode. Economic policy uncertainty (EPU) and, occasionally, trade policy uncertainty (TPU) display similar short-lived density increases. By late 2024, however, EPU shows both rising density and DY, consistent with a broader policy-uncertainty cycle around the U.S. election rather than a regional shock. TPU remains consistently secondary, with only transient upticks.

Taken together, the dual-metric evidence establishes a clear hierarchy of transmission channels. Episodes with *simultaneously high density and high DY*—as during the early-2022 surge in rates and volatility surrounding the Russia–Ukraine invasion—represent systemic stress, when shocks both synchronize markets and propagate dynamically across borders. By contrast, *high density with low DY*, exemplified by the October 2023 Hamas–Israel conflict, reflects a common geopolitical shock that triggered widespread repricing but without durable contagion. Finally, *moderate DY with low density*, evident in the run-up to the 2024 U.S. election as policy uncertainty rose, corresponds to directional spillovers through policy channels without full synchronization of global markets.

The overarching pattern is that global financial conditions—rates and volatility—anchor the baseline level of interconnectedness, ensuring that shocks in these domains reverberate broadly and persistently. Geopolitical and policy-related uncertainty, while influential, act mainly as episodic amplifiers: they generate sharp but typically transient co-movements unless reinforced by global financial tightening. The hierarchy is therefore clear: global financial shocks set the systemic baseline, domestic uncertainty transmits through narrower channels, and geopolitical events add volatility but rarely sustain contagion. This framework highlights the primacy of the global financial cycle in shaping sovereign risk linkages, with political and policy shocks exerting second-order, state-dependent effects.

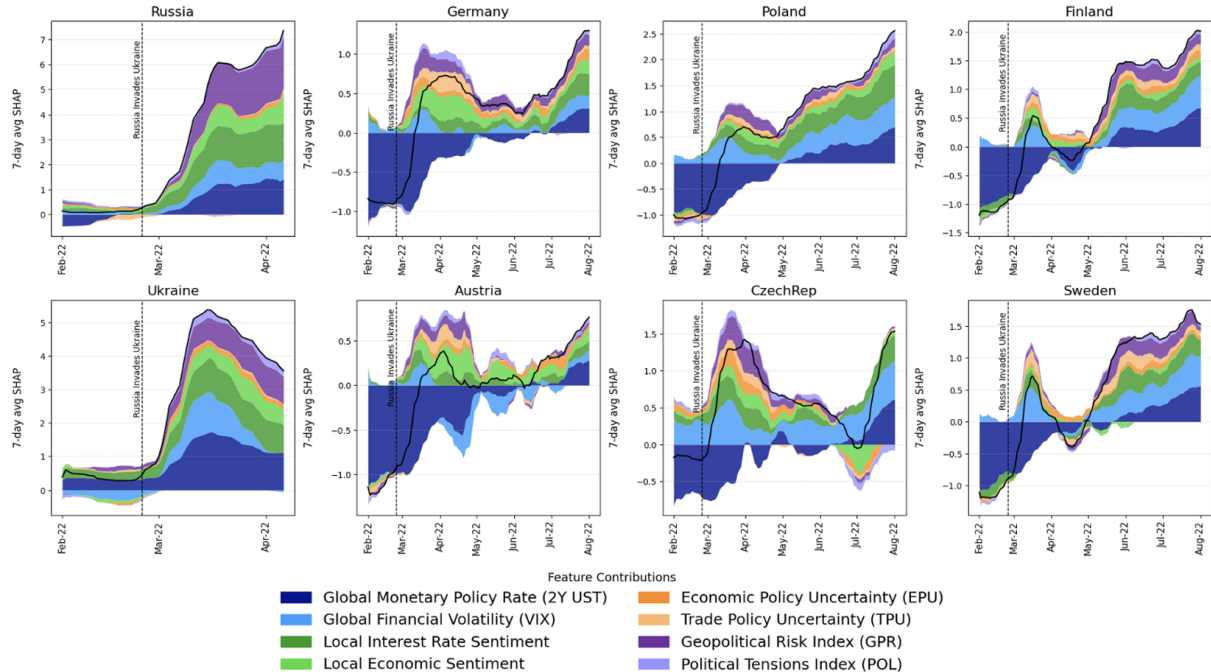
5 The Impact of Geopolitical and Geoeconomic Shocks on Sovereign Risk

In an increasingly fragmented world, understanding how geopolitical and geoeconomic shocks transmit to sovereign risk is paramount. We analyze three real-world events—an interstate war (Russia–Ukraine), a localized conflict with limited global reach (Hamas–Israel), and a geoeconomic trade shock (U.S. tariffs)—using the evolution of Shapley values. By virtue of *local accuracy* and *consistency*, Shapley values decompose day-by-day changes in model-predicted sovereign risk into positive and negative contributions by each driver, allowing us to trace transmission channels with precision. These case studies provide concrete illustrations of the patterns documented in the SHAP relevance and network analysis: Russia–Ukraine corresponds to a systemic stress episode (high density and spillovers), Hamas–Israel exemplifies a localized common shock with limited contagion, and the U.S. tariff conflict reflects a geoeconomic shock transmitted both through trade partners and via global financial volatility.

5.1 Geopolitical Shock: The Russia–Ukraine War

The February 24, 2022 invasion illustrates how a regional conflict can escalate into a systemic macro-financial shock. Figure 9 shows that spreads for the direct combatants (Russia and Ukraine) spiked sharply. For Russia, the surge reflects not only Geopolitical Risk (GPR) but also a rapid deterioration in domestic conditions and, subsequently, tighter global financial conditions. Sanctions and market exclusion magnified these pressures, consistent with evidence that conflict episodes raise sovereign spreads and volatility (Caldara and Iacoviello, 2022; Boubaker et al., 2023). For Ukraine, spreads increased immediately as geopolitical premia combined with broad-based declines in domestic conditions and heightened policy uncertainty, in line with historical findings on war shocks (Caldara and Iacoviello, 2022).

Figure 9: Shapley contribution changes to sovereign risk after the Russian invasion of Ukraine



Notes: Figure 8 plots the evolution of Shapley contributions to sovereign CDS spreads for selected countries before and after February 2022. For Russia and Ukraine, contributions from global drivers (global monetary policy rates, global financial volatility) and geopolitical risk measures surge. For European economies (Germany, Poland, Finland, Austria, Czech Republic, Sweden), the impact is more moderate but still material, with local sentiment and policy uncertainty amplifying exposure. Global financial conditions remain the dominant explanatory factor, while geopolitical and political tensions add substantial power for directly exposed countries.

Among European neighbors, GPR rose broadly but milder; Economic Policy Uncertainty (EPU) and Trade Policy Uncertainty (TPU) also increased, reflecting proximity and energy dependence. The most salient dynamic is the swift deterioration first in global policy rates and then in global financial volatility. Major central banks (including the

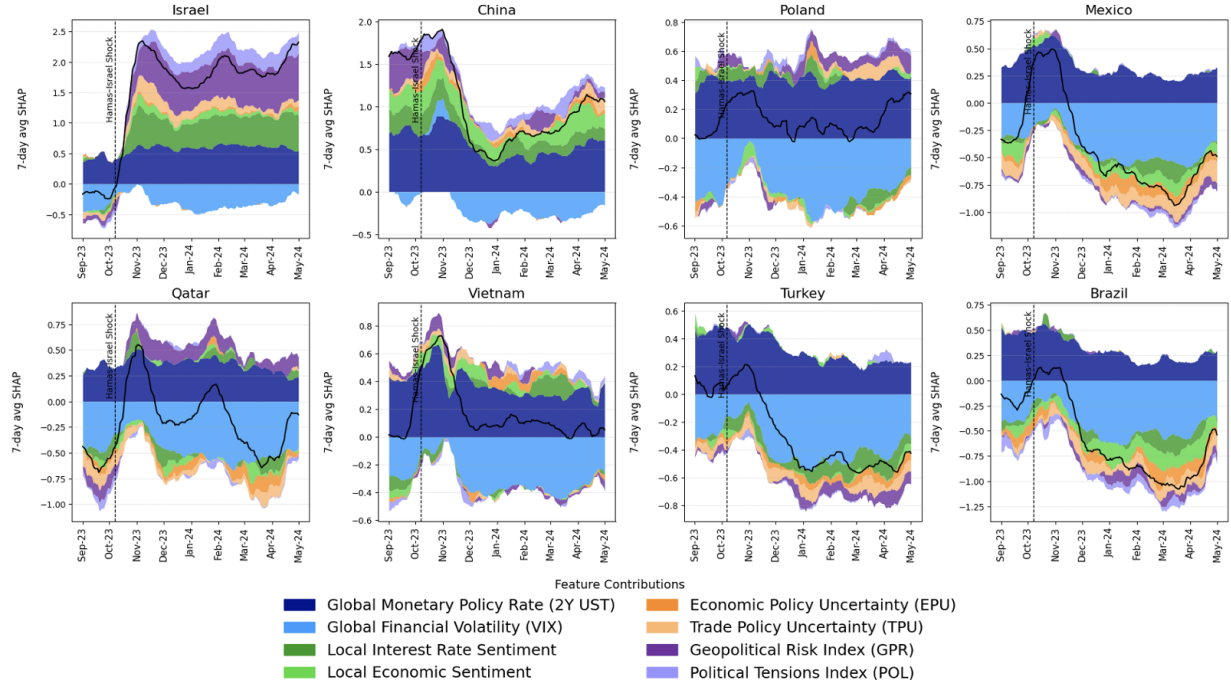
Federal Reserve and the ECB) pivoted from accommodation to tightening roughly three months after the shock, lifting funding costs and depressing risk appetite. The initial spike in GPR was thus quickly overshadowed by rising policy uncertainty and, in many cases, by the stronger influence of global monetary policy. Reliance on Russian energy and supply-chain disruptions amplified the inflation and uncertainty channels, transforming the geopolitical shock into a broader macro-financial one once central banks reacted to the inflation impulse (Novta and Pugacheva, 2021). According to ECB officials, “the Russian invasion of Ukraine in February 2022 was a distinct additional shock that accounted for most of the extraordinary surge in inflation during 2022, especially in Europe” (Lane, 2024). Given the nonlinear nature of inflation dynamics, this implies the war was pivotal in turning already elevated post-pandemic pressures into an “extraordinary surge.”

Taken together, the evidence reveals a cascade: geopolitical shock → commodity and inflation shock → policy uncertainty → global financial tightening—an evolution from localized conflict to systemic geoeconomic stress, reinforcing the global financial cycle (Bloom, 2009; Rey, 2013; Aiyar et al., 2023).

5.2 Geopolitical Shock: The Hamas–Israel Conflict

By contrast, the October 2023 Hamas–Israel conflict was a *localized* geopolitical shock. Figure 10 shows that for *Israel* the effect was immediate and persistent, driven primarily by geopolitical factors alongside weakening domestic conditions and rising policy/trade uncertainty, consistent with conflict risk being priced directly in the affected sovereign (Caldara and Iacoviello, 2022). Neighboring economies (e.g., *Qatar*, *Turkey*) experienced muted increases in geopolitical contributions, indicating contained regional spillovers; for most other EMs (e.g., *Mexico*, *Brazil*, *Poland*) and major Asian economies (*China*, *Vietnam*), GPR remained flat, underscoring the limited systemic reach (Novta and Pugacheva, 2021).

Figure 10: Shapley contribution changes to sovereign risk after the Hamas–Israel attack and response



Notes: The figure plots Shapley contributions to sovereign CDS spreads after October 2023. For Israel, geopolitical risk and political tensions dominate, with heightened global volatility. Qatar and Turkey show increases in geopolitical/political contributions but remain secondary to global drivers. For non-regional economies (China, Vietnam, Mexico, Poland, Brazil), global financial conditions (monetary policy, volatility) remain primary; geopolitical spillovers are limited.

Crucially, the conflict coincided with signals that the global tightening cycle was ending.¹³ As policy-rate expectations softened and volatility receded, global financial conditions shifted from amplifying sovereign risk to supporting a broad-based decline in premia, offsetting contagion outside the region. This interaction between a localized conflict and an accommodative global cycle helps explain the limited global impact (Rey, 2013; Bloom, 2009).

5.3 Geoeconomic Shock: Trump Election and U.S. Tariffs

The 2024 U.S. presidential election and subsequent tariff measures constitute a *geoeconomic* shock transmitted through trade and policy uncertainty. The response unfolded in two phases: the election in November 2024 and the tariff implementation in early 2025 (“Liberation Day,” April 2, 2025). Initially, EPU and TPU contributions spiked in the United States and key trading partners (Canada, Mexico, China), reflecting heightened policy unpredictability.¹⁴ For many other EMs, immediate effects were more muted and transmitted primarily via global uncertainty. Some countries (e.g., Mexico) also saw geopolitical contributions rise, reflecting concurrent rhetoric on immigration and security; China and Poland show modest GPR deterioration as well.

With tariff announcements and implementation, uncertainty crystallized into a concrete *geoeconomic* shock. For the United States, China, Mexico, and Canada, EPU/TPU contributions became dominant drivers of sovereign risk, consistent with evidence that protectionism and sanctions destabilize credit premia (Ahn and Ludema, 2020; Itsikhoki and Ribakova, 2024). For other EMs (e.g., Poland, Turkey, Brazil, Vietnam), effects were indirect: tariffs raised global volatility and altered monetary expectations, transmitting risk through the global financial channel rather than direct trade exposure (Glick and Rose, 1999; Diebold and Yilmaz, 2012a).

In sum, this episode exemplifies a geoeconomic scenario: policy uncertainty materializes as tariffs, reshaping sovereign risk both directly (via trade exposure) and indirectly (via global financial conditions).

5.4 Comparing the Three Episodes

The three cases reveal systematic differences in shock type, transmission, and interaction with the global financial cycle:

- *Nature of the shock.* Russia–Ukraine and Hamas–Israel are *geopolitical* shocks dominated by GPR; both show country-level deteriorations in domestic conditions and uncertainty for directly affected sovereigns, consistent with recent evidence on household and firm responses to geopolitical risk (Gorodnichenko et al., 2025).¹⁵ The tariff episode is *geoeconomic*, driven largely by EPU/TPU and prospective policy responses to the inflationary effects of trade restrictions.
- *Primary transmission channel.* Russia–Ukraine propagated via *proximity* and then via *energy/inflation* into broader macro-financial stress. Hamas–Israel remained largely *regional*, with the global footprint transmitted mainly through the *global financial channel* (VIX, policy expectations) in an easing environment. Tariffs propagated through a *direct trade channel* for the U.S. and core partners, while raising volatility and shifting monetary expectations for others.
- *Nonlinear interaction with the global financial cycle (rates and volatility).* Global conditions were decisive but state-dependent. In Russia–Ukraine, the war *exacerbated* an ongoing inflation impulse, prompting aggressive tightening. In Hamas–Israel, a dovish pivot *offset* broader contagion. In the tariff case, the trade shock itself *triggered* tighter global financial conditions by raising volatility and altering policy-rate expectations. These patterns align with the primacy of the *global financial cycle* (Rey, 2013) and the amplification of uncertainty under financial stress (Bloom, 2009).

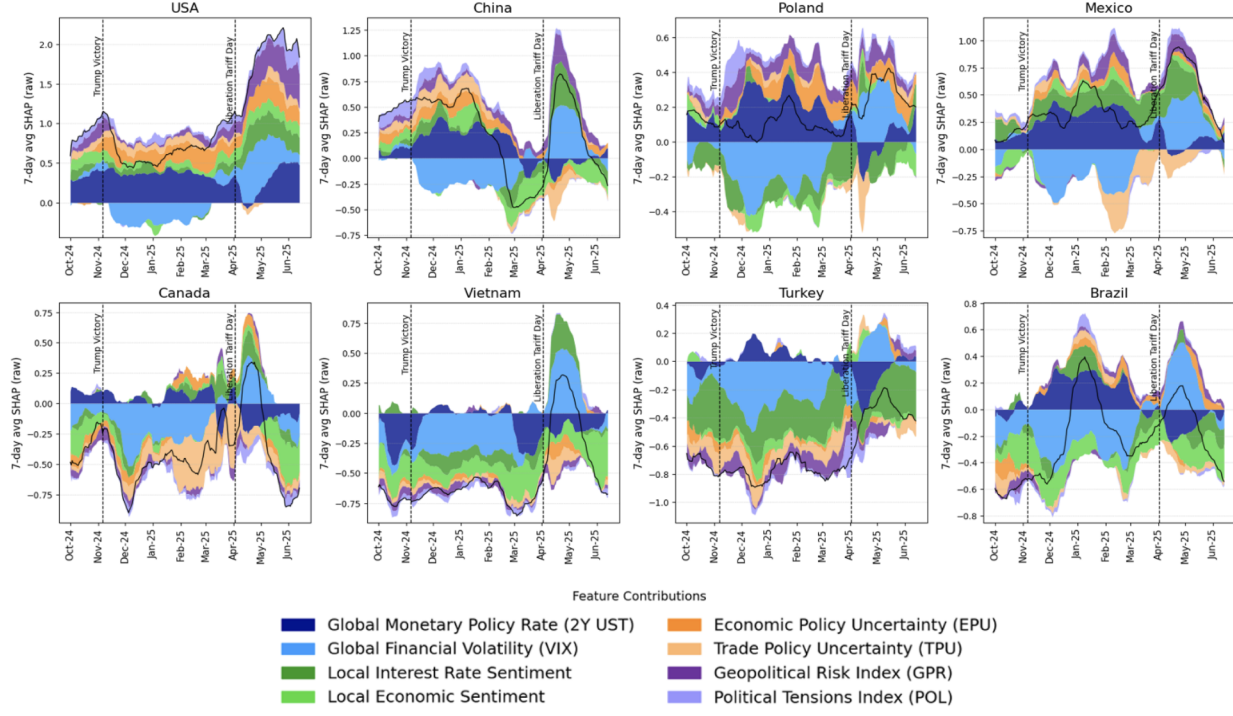
Overall, the global impact of shocks depends critically on their interaction with the *global financial cycle*, which governs whether effects are amplified, muted, or offset.

¹³By October 2023, the Federal Reserve had held the funds rate at 5.25–5.50% since July and noted in its 2023 Monetary Policy Report that policy was “likely at its peak for this tightening cycle” (Federal Reserve, 2023a). The September 2023 FOMC minutes also emphasized caution and data dependence (Federal Reserve, 2023b).

¹⁴Implementation was erratic: a sweeping 25% tariff threat on all imports from Canada and Mexico (Feb 1, 2025) was quickly amended to exempt USMCA-compliant sectors (e.g., autos), highlighting policy volatility.

¹⁵Gorodnichenko et al. (2025) document that higher perceived conflict durations raise expectations of stagflation, worsen views on public finances and household conditions, and depress consumption, complementing evidence on adverse firm outcomes.

Figure 11: Shapley contribution changes to sovereign risk after Trump election and tariff policy



Notes: The figure shows Shapley contribution dynamics around the 2024 U.S. election and subsequent tariff announcements. For the United States, sovereign risk increases after the election and accelerates with tariff measures, driven by TPU, EPU, and global volatility. Spillovers are evident in Mexico, Canada, China, and Brazil through trade/policy uncertainty. For other economies (Poland, Turkey, Vietnam), global financial drivers remain central, with uncertainty effects rising around tariff dates. The evidence supports dual transmission: direct trade exposure for core participants and broader amplification through global financial volatility.

6 Conclusion

This study shows that sovereign risk is shaped by a complex interaction between global financial conditions, domestic sentiment, and geopolitical or policy-related uncertainty. Using high-frequency data and machine learning methods, we find that *non-linear models—particularly ensemble approaches—substantially outperform linear benchmarks in predicting sovereign CDS spreads*. This underscores the importance of accounting for threshold effects, asymmetries, and state dependence in financial markets.

We show that text-based indicators capture dimensions of sovereign risk not fully reflected in contemporaneous financial variables, and that their predictive value is inherently non-linear. The gains from incorporating news are modest in linear frameworks but become substantial when models allow for complex interactions. This highlights that the value of news lies not only in their inclusion but in how they are integrated, underscoring the importance of model choice in exploiting high-frequency, unstructured data.

We also provide a *structural reading of sovereign risk drivers through Shapley value decompositions*. Global monetary policy and financial volatility emerge as dominant “push” factors, consistent with the global financial cycle literature. Domestic sentiment and interest rate expectations differentiate risk across countries, while geopolitical and policy uncertainty play secondary but meaningful roles. Scenario analysis highlights that uncertainty shocks alone are modest, but when combined with global tightening, they generate powerful non-linear amplifications.

In addition, we introduce a joint perspective on interconnectedness by combining Diebold–Yilmaz spillovers with network density. *Global financial conditions (the U.S. 2-year rate and the VIX) emerge as the most persistent transmitters of sovereign risk*. Local macro sentiment amplifies shocks during stress episodes but later decouples, while *geopolitical and policy uncertainty factors generate sharp, episodic co-movements with limited sustained spillovers*.

Our final contribution is to document *heterogeneity across regions and asset classes*. Advanced economies are especially sensitive to shifts in global monetary policy, while emerging markets, particularly in Latin America and Asia, are

disproportionately exposed to volatility. Geopolitical risk is especially salient in the Middle East and Emerging Europe, reflecting structural vulnerabilities. Case studies of the Russia–Ukraine war, the Hamas–Israel conflict, and the U.S. tariff escalation illustrate these mechanisms in real time: systemic stress, localized common shocks, and geoeconomic trade shocks, respectively.

Taken together, the findings emphasize that sovereign risk cannot be understood in a purely global framework but requires accounting for regional exposures, institutional characteristics, and the interaction between news shocks and the global financial cycle. For policymakers, this implies that vulnerability management depends as much on external financial conditions as on domestic fundamentals, and that monitoring text-based indicators can provide timely warnings of amplifying shocks. Future research should explore how these high-frequency, non-linear interactions can be incorporated into sovereign risk surveillance and early-warning systems.

References

Ahir, H., Bloom, N., and Furceri, D. (2018). The world uncertainty index. *Brookings Papers on Economic Activity*, pages 343–400.

Ahn, D. P. and Ludema, R. D. (2020). The sword and the shield: The economics of targeted sanctions. *European Economic Review*, 130:103578.

Aiyar, S., Presbitero, A. F., and Ruta, M. (2023). Geoeconomic fragmentation and the future of multilateralism. IMF Staff Discussion Note SDN/2023/001, International Monetary Fund.

Alter, A. and Beyer, A. (2014). The dynamics of spillover effects during the european sovereign debt turmoil. *Journal of Banking and Finance*, 42:134–153.

Athey, S. and Imbens, G. W. (2019). Machine learning methods that economists should know about. *Annual Review of Economics*, 11(1):685–725.

Athey, S., Tibshirani, J., and Wager, S. (2018). Generalized random forests. *Annals of Statistics*.

Baker, S. R., Bloom, N., and Davis, S. J. (2016). Measuring economic policy uncertainty. *The Quarterly Journal of Economics*, 131(4):1593–1636.

Bank for International Settlements (2022). Bis annual economic report 2022. Technical report, Bank for International Settlements.

Barabási, A.-L. (2016). *Network Science*. Cambridge University Press.

Battiston, S., Caldarelli, G., May, R. M., Roukny, T., and Stiglitz, J. E. (2016). The price of complexity in financial networks. *Proceedings of the National Academy of Sciences*, 113(36):10031–10036.

Bekaert, G., Hoerova, M., and Lo Duca, M. (2013). Risk, uncertainty and monetary policy. *Journal of Monetary Economics*, 60(7):771–788.

Benchimol, J. and Palumbo, L. (2024). Sanctions and russian online prices. *Journal of Economic Behavior & Organization*, 225:483–521.

Bloom, N. (2009). The impact of uncertainty shocks. *Econometrica*, 77(3):623–685.

Bluwstein, K., Buckmann, M., Kapadia, S., and Stockdale, O. (2023). Systemic risk and financial spillovers: A machine learning approach. *Journal of Monetary Economics*, 134:80–99.

Bondarenko, Y., Lewis, V., Rottner, M., and Schüler, Y. (2024). Geopolitical risk perceptions. *Journal of International Economics*, 152:104005.

Boubaker, S., Goodell, J. W., Kumar, S., and Sureka, R. (2023). Geopolitical risk and energy stock performance: Evidence from the Russia–Ukraine conflict. *Journal of Commodity Markets*, 30:100325.

Breiman, L. (2001). Random forests. *Machine Learning*, 45(1):5–32.

Bruno, V. and Shin, H. S. (2015). Capital flows and the risk-taking channel of monetary policy. *Journal of Monetary Economics*, 71:119–132.

Caldara, D. and Iacoviello, M. (2022). Measuring geopolitical risk. *American Economic Review*, 112(4):1194–1225.

Caldara, D., Iacoviello, M., Molligo, P., Prestipino, A., and Raffo, A. (2020). The economic effects of trade policy uncertainty. *Journal of Monetary Economics*, 109:38–59.

Calvo, G. A., Izquierdo, A., and Mejía, L.-F. (2004). On the empirics of sudden stops: The relevance of balance-sheet effects. *NBER Working Paper*. NBER Working Paper No. 10520.

Calvo, G. A., Leiderman, L., and Reinhart, C. M. (1993). Capital inflows and real exchange rate appreciation in latin america: The role of external factors. *IMF Staff Papers*, 40(1):108–151.

Calvo, G. A., Leiderman, L., and Reinhart, C. M. (1996). Inflows of capital to developing countries in the 1990s. *Journal of Economic Perspectives*, 10(2):123–139.

Cont, R. (2001). Empirical properties of asset returns: stylized facts and statistical issues. *Quantitative Finance*, 1(2):223–236.

Davis, S. J., Hansen, S., and Seminario-Amez, C. (2025). Macro shocks and firm-level response heterogeneity. Working Paper.

Didier, T., Hevia, C., and Schmukler, S. L. (2012). Financial globalization in emerging economies: Much ado about nothing? *Journal of Development Economics*, 98(1):86–104.

Diebold, F. X. and Yilmaz, K. (2012a). Better to give than to receive: Predictive directional measurement of volatility spillovers. *International Journal of Forecasting*, 28(1):57–66.

Diebold, F. X. and Yilmaz, K. (2012b). Better to give than to receive: Predictive measurement of volatility spillovers. *International Journal of Forecasting*, 28(1):57–66.

Diebold, F. X. and Yilmaz, K. (2014). On the network topology of variance decompositions: Measuring the connectedness of financial firms. *Journal of Econometrics*, 182(1):119–134.

Eichengreen, B., Mody, A., Nedeljkovic, M., and Sarno, L. (2021). How global financial cycles and domestic fundamentals interact. *Journal of International Economics*, 132:103509.

Fernández, A., González, A., and Rodríguez, D. (2018). Commodity price synchronicity and financial variables. *Journal of International Financial Markets, Institutions and Money*, 56:26–40.

Fernández-Villaverde, J., Li, Y., Xu, L., and Zanetti, F. (2025). Charting the uncharted: The (un)intended consequences of oil sanctions and dark shipping. Working Paper 33486, National Bureau of Economic Research.

Fernandez-Villaverde, J., Mineyama, T., and Song, D. (2024). Are we fragmented yet? measuring geopolitical fragmentation and its causal effects. Working Paper 32638, National Bureau of Economic Research.

Fratzscher, M. (2012). Capital flows, push versus pull factors and the global financial crisis. *Journal of International Economics*, 88(2):341–356.

Friedman, J. H. (2001). Greedy function approximation: A gradient boosting machine. *Annals of Statistics*, 29(5):1189–1232.

Gelos, R. G., Sahay, R., and Sandleris, G. (2011). Sovereign borrowing by developing countries: What determines the bond spread? *Journal of Development Economics*, 96(2):273–282.

Gentzkow, M., Kelly, B., and Taddy, M. (2019). Text as data. *Journal of Economic Literature*, 57(3):535–574.

Glick, R. and Rose, A. K. (1999). Contagion and trade: why are currency crises regional? *Journal of International Money and Finance*, 18(4):603–617.

Gorodnichenko, Y., Georgarakos, D., Kenny, G., and Coibion, O. (2025). The Impact of Geopolitical Risk on Consumer Expectations and Spending. Technical Report w34195, National Bureau of Economic Research.

Goulet Coulombe, P., Leroux, M., Stevanovic, D., and Surprenant, S. (2022). How is machine learning useful for macroeconomic forecasting? *Journal of Applied Econometrics*, 37(5):920–964.

Gu, S., Kelly, B. T., and Xiu, D. (2020). Empirical asset pricing via machine learning. *The Review of Financial Studies*, 33(5):2223–2273.

Hamilton, J. D. (1989). A new approach to the economic analysis of nonstationary time series and the business cycle. *Econometrica*, 57(2):357–384.

Hassan, T. A., Hollander, S., van Lent, L., and Tahoun, A. (2019). Firm-level political risk: Measurement and effects. *The Quarterly Journal of Economics*, 134(4):2135–2202.

Hastie, T., Tibshirani, R., and Friedman, J. (2009). *The Elements of Statistical Learning: Data Mining, Inference, and Prediction*. Springer Series in Statistics. Springer, second edition.

Hoerl, A. E. and Kennard, R. W. (1970). Ridge regression: Biased estimation for nonorthogonal problems. *Technometrics*, 12(1):55–67.

International Monetary Fund (2019). Global financial stability report: Lower for longer. Technical report, International Monetary Fund, Washington, D.C.

International Monetary Fund (2022). Global financial stability report. Technical report, International Monetary Fund.

Itskhoki, O. and Ribakova, E. (2024). The economics of sanctions: From theory into practice. Technical report, Brookings Institution. Brookings Papers on Economic Activity Conference Draft.

Jolliffe, I. T. (2002). *Principal Component Analysis*. Springer Series in Statistics. Springer, second edition.

Joseph, A. and Strobel, F. (2021). Machine learning for financial crises prediction: An empirical comparison with linear models. *Journal of Financial Stability*, 56:100939.

Koenker, R. and Bassett, G. (1978). Regression quantiles. *Econometrica*, 46(1):33–50.

Lane, P. R. (2024). The ecb, inflation and the ukraine shock. European Central Bank Blog. Accessed: 2025-09-04.

LeCun, Y., Bengio, Y., and Hinton, G. (2015). Deep learning. *Nature*, 521(7553):436–444.

Leetaru, K. and Schrottd, P. A. (2013). Gdelt: Global data on events, location, and tone, 1979–2012. Technical Report Version 1.0, GDELT Project. Presented at the International Studies Association Annual Convention, San Francisco, CA.

Lundberg, S. M. and Lee, S.-I. (2017). A unified approach to interpreting model predictions. In Advances in Neural Information Processing Systems, volume 30, pages 4765–4774.

Manela, A. and Moreira, A. (2017). News implied volatility and disaster concerns. *Journal of Financial Economics*, 123(1):137–162.

Miranda-Agrippino, S. and Rey (2020). U.S. Monetary Policy and the Global Financial Cycle. *The Review of Economic Studies*, 87(6):2754–2776.

Molnar, C. (2019). *Interpretable Machine Learning: A Guide for Making Black Box Models Explainable*. Lulu.com.

Mueller, H. and Rauh, C. (2018). Reading between the lines: Prediction of political violence using newspaper text. *American Political Science Review*, 112(2):358–375.

Mueller, H. and Rauh, C. (2022). Using past violence and current news to predict changes in violence. *International Interactions*, 48(4):579–596.

Mullainathan, S. and Spiess, J. (2017). Machine learning: An applied econometric approach. *Journal of Economic Perspectives*, 31(2):87–106.

Newman, M. (2010). *Networks: An Introduction*. Oxford University Press.

Novta, N. and Pugacheva, E. (2021). Geopolitical risks and capital flows to emerging markets. *Journal of International Money and Finance*, 115:102391.

O’Malley, T., Bursztein, E., Long, J., Chollet, F., Jin, H., Invernizzi, L., et al. (2019). Kerastuner. GitHub repository.

Reinhart, C. M., Rogoff, K. S., and Savastano, M. A. (2003). Debt intolerance. *Brookings Papers on Economic Activity*, 2003(1):1–74.

Rey, H. (2013). Dilemma not trilemma: The global financial cycle and monetary policy independence. *Proceedings of the Jackson Hole Economic Policy Symposium*, pages 285–333.

Ribeiro, M. T., Singh, S., and Guestrin, C. (2016). Why should i trust you? explaining the predictions of any classifier. In *Proceedings of the 22nd ACM SIGKDD International Conference on Knowledge Discovery and Data Mining*, pages 1135–1144.

Shapley, L. S. (1953). A value for n-person games. *Contributions to the Theory of Games*, 2:307–317.

Stock, J. H. and Watson, M. W. (2002). Forecasting using principal components from a large number of predictors. *Journal of the American Statistical Association*, 97(460):1167–1179.

Stock, J. H. and Watson, M. W. (2003). *Introduction to Econometrics*. Addison-Wesley, first edition.

Swanson, E. T. (2021). Measuring the effects of federal reserve forward guidance and large-scale asset purchases on financial markets. *American Economic Review*, 111(11):3655–3695.

Teräsvirta, T. (1994). Specification, estimation, and evaluation of smooth transition autoregressive models. *Journal of the American Statistical Association*, 89(425):208–218.

Tibshirani, R. (1996). Regression shrinkage and selection via the lasso. *Journal of the Royal Statistical Society, Series B (Methodological)*, 58(1):267–288.

Varian, H. R. (2014). Big data: New tricks for econometrics. *Journal of Economic Perspectives*, 28(2):3–28.

Zou, H. and Hastie, T. (2005). Regularization and variable selection via the elastic net. *Journal of the Royal Statistical Society, Series B (Methodological)*, 67(2):301–320.

A APPENDIX A: The data

This annex details country-specific data availability, as well as percentile distributions by country (Appendix A.1), as well as the procedures employed for the construction of the news-based indicators used in the empirical analysis (Appendix A.2).

A.1 Data availability by country

We include a summary describing the basis for the empirical analysis developed in the paper. Table XX presents country-specific data availability together with descriptive statistics summarizing the distribution of the main variables. For each country, the start and end dates of the available sample are reported. To characterize the distribution, we provide the 25th and 75th percentiles (p25 and p75), which capture the interquartile range where the central 50% of observations lie, for each of the described variables in the data section.

Figure 12: Country-specific sample periods and interquartile distributions of variables

Country	Sample		CDS	Global financial var.				Macroeconomic sentiment var.								Political and Geop. var.					
	Start	End		p25	p75	FED	VIX	ECO	INT	EPU	TPU	p25	p75	p25	p75	p25	p75	GPR	POL		
	11/08/2020	13/06/2025	-0.78	0.77	-1.30	0.79	-0.72	0.60	-0.72	0.77	-0.39	0.68	-0.68	0.29	-0.77	0.66	-0.82	0.70	-0.76	0.52	
Argentina	11/08/2020	13/06/2025	-0.64	0.66	-1.03	0.99	-0.71	0.41	-0.34	0.61	-0.49	0.70	-0.65	0.30	-0.63	0.41	-0.69	0.58	-0.72	0.58	
Australia	01/01/2018	13/06/2025	-0.95	0.64	-1.03	0.99	-0.71	0.41	-0.39	0.61	-0.39	0.66	-0.64	0.27	-0.56	0.21	-0.57	0.33	-0.69	0.61	
Austria	01/01/2018	13/06/2025	-0.82	0.63	-1.03	0.99	-0.71	0.41	-0.34	0.64	-0.36	0.67	-0.69	0.48	-0.71	0.53	-0.58	0.44	-0.67	0.45	
Belgium	01/01/2018	13/06/2025	-0.73	0.66	-1.03	0.99	-0.71	0.41	-0.37	0.67	-0.38	0.67	-0.76	0.57	-0.76	0.52	-0.70	0.57	-0.72	0.47	
Brazil	01/01/2018	13/06/2025	-0.65	0.43	-1.03	0.99	-0.71	0.41	-0.62	0.72	-0.52	0.55	-0.73	0.54	-0.69	0.60	-0.67	0.54	-0.85	0.61	
Canada	21/02/2019	14/06/2025	-0.82	0.78	-1.19	0.96	-0.68	0.44	-0.41	0.68	-0.36	0.68	-0.54	0.16	-0.44	-0.05	-0.72	0.61	-0.75	0.57	
Chile	01/01/2018	13/06/2025	-0.79	0.57	-1.03	0.99	-0.71	0.41	-0.73	0.79	-0.50	0.76	-0.64	0.37	-0.58	0.45	-0.75	0.58	-0.55	0.52	
China	01/01/2018	13/06/2025	-0.91	0.67	-1.03	0.99	-0.71	0.41	-0.29	0.58	-0.21	0.50	-0.75	0.54	-0.67	0.52	-0.69	0.49	-0.74	0.66	
Colombia	01/01/2018	13/06/2025	-0.78	0.80	-1.03	0.99	-0.71	0.41	-0.45	0.54	-0.04	0.34	-0.68	0.45	-0.69	0.69	-0.70	0.44	-0.68	0.57	
CzechRep	01/01/2018	13/06/2025	-0.74	0.49	-1.03	0.99	-0.71	0.41	-0.50	0.50	-0.29	0.60	-0.72	0.46	-0.70	0.51	-0.64	0.45	-0.62	0.41	
Denmark	01/01/2018	13/06/2025	-0.74	0.30	-1.03	0.99	-0.71	0.41	-0.44	0.56	-0.33	0.51	-0.68	0.54	-0.67	0.58	-0.75	0.49	-0.66	0.47	
Egypt	01/01/2018	13/06/2025	-0.79	0.80	-1.03	0.99	-0.71	0.41	-0.46	0.69	-0.57	0.73	-0.68	0.47	-0.70	0.49	-0.70	0.48	-0.58	0.51	
Finland	01/01/2018	13/06/2025	-0.78	0.55	-1.03	0.99	-0.71	0.41	-0.29	0.60	-0.36	0.61	-0.49	0.10	-0.67	0.47	-0.60	0.44	-0.79	0.59	
France	01/01/2018	13/06/2025	-0.69	0.34	-1.03	0.99	-0.71	0.41	-0.41	0.66	-0.38	0.66	-0.67	0.36	-0.72	0.58	-0.61	0.40	-0.69	0.59	
Germany	01/01/2018	13/06/2025	-0.75	0.52	-1.03	0.99	-0.71	0.41	-0.50	0.64	-0.15	0.56	-0.69	0.55	-0.71	0.48	-0.57	0.31	-0.60	0.49	
Hungary	01/01/2018	13/06/2025	-0.59	0.47	-1.03	0.99	-0.71	0.41	-0.46	0.63	-0.42	0.71	-0.67	0.38	-0.69	0.47	-0.66	0.46	-0.75	0.59	
India	01/01/2018	13/06/2025	-0.72	0.42	-1.03	0.99	-0.71	0.41	-0.64	0.63	-0.28	0.62	-0.62	0.25	-0.61	0.38	-0.66	0.58	-0.67	0.60	
Indonesia	01/01/2018	13/06/2025	-0.75	0.17	-1.03	0.99	-0.71	0.41	-0.49	0.74	-0.38	0.70	-0.69	0.51	-0.52	-0.06	-0.74	0.57	-0.86	0.59	
Israel	01/01/2018	13/06/2025	-0.83	0.58	-1.03	0.99	-0.71	0.41	-0.43	0.74	-0.17	0.61	-0.79	0.58	-0.54	0.09	-0.62	0.44	-0.63	0.37	
Italy	01/01/2018	13/06/2025	-0.71	0.47	-1.03	0.99	-0.71	0.41	-0.42	0.68	-0.40	0.68	-0.75	0.58	-0.75	0.45	-0.73	0.52	-0.70	0.38	
Japan	27/10/2023	13/06/2025	-0.63	0.55	-0.83	0.87	-0.76	0.41	-0.64	0.49	-0.36	0.64	-0.65	0.26	-0.73	0.65	-0.78	0.59	-0.63	0.63	
Jordan	01/01/2018	13/06/2025	-0.78	0.57	-1.03	0.99	-0.71	0.41	-0.64	0.63	-0.28	0.62	-0.62	0.25	-0.61	0.38	-0.84	0.69	-0.68	0.68	
Malaysia	01/01/2018	13/06/2025	-0.66	0.34	-1.03	0.99	-0.71	0.41	-0.35	0.64	-0.27	0.60	-0.72	0.66	-0.59	0.19	-0.69	0.58	-0.64	0.53	
Mexico	01/01/2018	13/06/2025	-0.56	0.17	-1.03	0.99	-0.71	0.41	-0.56	0.52	-0.16	0.42	-0.74	0.61	-0.69	0.62	-0.68	0.52	-0.66	0.58	
Morocco	01/01/2018	13/06/2025	-0.79	0.35	-1.03	0.99	-0.71	0.41	-0.70	0.72	-0.32	0.64	-0.74	0.51	-0.74	0.52	-0.64	0.49	-0.67	0.43	
Netherlands	01/01/2018	13/06/2025	-0.71	0.44	-1.03	0.99	-0.71	0.41	-0.45	0.73	-0.27	0.62	-0.70	0.38	-0.63	0.14	-0.65	0.57	-0.80	0.66	
Norway	01/01/2018	13/06/2025	-0.53	0.37	-1.03	0.99	-0.71	0.41	-0.39	0.60	-0.31	0.62	-0.59	0.22	-0.64	0.45	-0.60	0.43	-0.64	0.36	
Peru	01/01/2018	13/06/2025	-0.78	0.69	-1.03	0.99	-0.71	0.41	-0.52	0.75	-0.20	0.54	-0.61	0.35	-0.71	0.51	-0.76	0.68	-0.69	0.45	
Philippines	01/01/2018	13/06/2025	-0.52	0.00	-1.03	0.99	-0.71	0.41	-0.45	0.69	-0.37	0.65	-0.74	0.51	-0.64	0.40	-0.71	0.50	-0.73	0.67	
Poland	01/01/2018	13/06/2025	-0.65	0.49	-1.03	0.99	-0.71	0.41	-0.65	0.49	-0.12	0.47	-0.64	0.25	-0.68	0.46	-0.75	0.36	-0.54	0.40	
Qatar	01/01/2018	13/06/2025	-0.65	0.49	-1.03	0.99	-0.71	0.41	-0.65	0.49	-0.12	0.47	-0.64	0.25	-0.68	0.46	-0.75	0.36	-0.54	0.40	
Russia	01/01/2018	06/04/2022	-0.21	-0.11	-1.08	1.02	-0.67	0.41	-0.36	-0.15	0.61	0.01	0.48	-0.76	0.51	-0.67	0.45	-0.50	0.36	-0.62	0.30
SaudiA.	01/01/2018	13/06/2025	-0.65	0.46	-1.03	0.99	-0.71	0.41	-0.42	0.56	-0.14	0.55	-0.76	0.53	-0.73	0.55	-0.73	0.57	-0.55	0.44	
Spain	01/01/2018	13/06/2025	-0.76	0.38	-1.03	0.99	-0.71	0.41	-0.35	0.65	-0.27	0.58	-0.65	0.39	-0.52	0.27	-0.63	0.41	-0.67	0.51	
Sweden	01/01/2018	13/06/2025	-0.71	0.83	-1.03	0.99	-0.71	0.41	-0.53	0.69	-0.41	0.68	-0.71	0.45	-0.45	0.11	-0.64	0.52	-0.76	0.60	
Thailand	01/01/2018	13/06/2025	-0.55	0.31	-1.03	0.99	-0.71	0.41	-0.44	0.72	-0.25	0.50	-0.60	0.36	-0.42	0.19	-0.68	0.43	-0.28	0.59	
Turkey	01/01/2018	13/06/2025	-0.77	0.73	-1.03	0.99	-0.71	0.41	-0.46	0.64	-0.20	0.53	-0.66	0.47	-0.68	0.50	-0.74	0.59	-0.47	0.56	
UK	01/01/2018	13/06/2025	-0.71	0.72	-1.03	0.99	-0.71	0.41	-0.39	0.69	-0.43	0.69	-0.65	0.44	-0.55	0.34	-0.62	0.39	-0.66	0.41	
USA	01/01/2018	13/06/2025	-0.79	0.76	-1.03	0.99	-0.71	0.41	-0.17	0.58	-0.45	0.70	-0.62	0.28	-0.69	0.41	-0.63	0.50	-0.72	0.51	
Ukraine	17/01/2020	06/04/2022	-0.33	-0.14	-0.54	0.09	-0.73	0.28	-0.41	0.70	0.15	0.47	-0.81	0.59	-0.72	0.47	-0.69	0.29	-0.67	0.67	
Uruguay	01/01/2018	13/06/2025	-0.75	0.45	-1.03	0.99	-0.71	0.41	-0.49	0.65	-0.48	0.69	-0.71	0.51	-0.62	0.59	-0.72	0.54	-0.79	0.65	
Vietnam	01/01/2018	13/06/2025	-0.69	0.40	-1.03	0.99	-0.71	0.41	-0.70	0.64	-0.60	0.66	-0.68	0.35	-0.65	0.26	-0.78	0.75	-0.23	0.56	

A.2 Media sentiment indicators development process

All indices are developed by BBVA Research using the Global Database of Events, Language, and Tone (GDELT) as described previously in the data section. The indices are daily and collected at the country level. To ensure homogeneity, each index is normalized (minus average and divided by standard deviation) and smoothed using a 28-day moving average. This transformation reduces daily noise and allows for a clearer identification of signals. No outlier treatment is performed, since the objective is to capture events that stand out from the normal behavior of the indicators.

The detailed set of keywords included in each case to build the indicators are the following:

- Economic Policy Uncertainty (EPU) Index

The Economic Policy Uncertainty (EPU) Index is originally constructed by BBVA Research based on the relative coverage associated with GDELT searches using country-specific keywords. The specific choice of keywords for each country aims to replicate the methodology presented by Baker, Bloom and Davis (2016) in "Measuring Economic Policy Uncertainty".

- United States: "United States (uncertainty OR uncertain) (economic OR economy) (congress OR legislation OR white house OR regulation OR federal reserve OR deficit)"
- China: "China (uncertain OR uncertainty) (economy OR economic OR business) (fiscal OR monetary OR Commission OR bank OR legislation OR tax OR bonds OR debt OR tariff OR deficit)"
- Canada: "Canada (uncertain OR uncertainty)(economic OR economy)(policy OR tax OR spending OR regulation OR central bank OR budget OR deficit)"
- Mexico: "Mexico (economic OR economy) (uncertain OR uncertainty) (regulation OR deficit OR budget OR Bank OR BdeM OR Banxico OR congress OR senate OR deputies OR legislation OR taxes OR Federal Reserve)"
- Spain: "Spain (uncertainty OR uncertain OR instability OR risk) (economic OR economy) (parliament OR government OR Hacienda OR deficit OR budget OR expenditure OR debt OR taxes OR law OR reform OR regulation OR Bank)"
- Australia: "Australia (uncertain OR uncertainty) (economic OR economy) (regulation OR Reserve Bank of Australia OR RBA OR deficit OR tax OR taxation OR taxes OR parliament OR senate OR cash rate OR legislation OR tariff OR war)"
- Brazil: "Brazil (uncertain OR uncertainty) (economic OR economy) (regulation OR deficit OR budget OR tax OR central bank OR Alvorada OR Planalto OR congress OR senate OR deputies OR legislation OR law OR tariff)"
- Chile: "Chile (uncertain OR uncertainty) (economic OR economy) (politics OR tax OR regulation OR reform OR congress OR senate OR spending OR debt OR budget OR Central Bank OR Ministry of Finance)"
- Colombia: "Colombia (economy OR economic) (uncertainty OR uncertain) (politics OR politician OR government OR tax OR reform OR deficit OR debt OR spending OR congress OR crisis OR Bank OR Ministry OR corruption OR peace OR conflict OR subsidy)"
- France: "France (uncertain OR uncertainty) (economic OR economy) (congress OR legislation OR regulation OR central bank OR ECB OR deficit)"
- Germany: "Germany (uncertain OR uncertainty) (economic OR economy) (congress OR legislation OR regulation OR central bank OR ECB OR deficit)"
- India: "India (uncertain OR uncertainty OR uncertainties) (economic OR economy) (regulation OR central bank OR monetary policy OR policymakers OR deficit OR legislation OR fiscal policy)"
- Pakistan: "Pakistan (uncertainty OR uncertain OR unpredictable OR unclear OR unstable) (economics OR economy) (regulation OR policy OR bank OR SBP OR FBR OR tax OR parliament OR deficit OR government OR reserves OR taxes OR legislation)"
- Russia: "Russia (uncertain OR uncertainty) (economic OR economy) (policy OR tax OR spending OR regulation OR central bank OR law OR Duma OR budget)"
- Turkey: "Turkey (uncertain OR uncertainty) (economic OR economy)"
- United Kingdom: "(United Kingdom OR UK) (uncertain OR uncertainty) (economic OR economy) (policy OR tax OR spending OR regulation OR Bank of England OR budget OR deficit)"
- All other countries: "COUNTRY_NAME (uncertain OR uncertainty) (economic OR economy) (policy OR tax OR spending OR regulation OR central bank OR budget OR deficit)"

The constructed index corresponds to the relative coverage (number of news related to EPU / total number of published news). The indices are smoothed with a 28-day moving average and normalized.

- Political Tensions Index

The Political Tensions Index is originally constructed by BBVA Research based on the tone and coverage associated with GDELT searches of keywords for: political instability, political uncertainty, political crisis, political polarization, political extremism, political turmoil, political conflict. Additionally, the index uses the GDELT taxonomy USPEC_POLITICS_GENERAL1, which includes news related to: Elections and campaigns, Political parties and politicians, Government institutions and branches, Executive orders and presidential actions, Congressional activities and legislation, Supreme Court decisions and judicial appointments, Political scandals and corruption, Civil rights and social justice issues, Foreign policy and international relations, National security and defense policy, Immigration policy and border security, Healthcare policy and reform, Environmental policy and regulation, Tax policy and reform, Gun control and firearms policy, Education policy and reform, Infrastructure policy and investment, Social welfare policy and programs, Civil liberties and privacy concerns, Political polarization and partisanship.

The keywords contained in the query use “OR” statements so that the mention of any of them returns news articles containing any one of them, provided the articles are classified within the GDELT taxonomy theme USPEC_POLITICS_GENERAL1.

The index is a weighted product of tone (sentiment) and relative coverage and it is multiplied by -1 for interpretability.

- Geopolitical Risk (GPR) Index

The Geopolitical Risk Index is originally constructed by BBVA Research based on the tone and coverage associated with GDELT searches, following the methodology of Caldara and Iacoviello (2022).

The data should contain at least one theme included in the GDELT taxonomy of each group:

- Group 1: war, conflict, hostvisit, revolutionary violence, appraiser, rebellion, violent unrest, peacekeeping, mutual recognition agreements, ceasefire, treaties, parliament and legislatures, military, troop, nuclear-power, hydropower, terror, rebels guerrillas and insurgents, kidnap, alliance, group popular resistance committee, insurgency, group social resistance, military cooperation, navy, aerial photographer, rebels.
- Group 2: act harmthreaten, advertiser, risk, concern worldwide, speciesendangered, crisis, trouble, dispute boards, dismissal procedures, boycott, disruption, slfid military buildup, sanctions, blockade, financial vulnerability and risks, soc quarantine, unrest ultimatum, makestatement, outbreak, announcer, armourer, persecution, crash, raid, armedconflict, act forceposttrue, bombthreat, kill, strike.

The index is a weighted product of tone (sentiment) and relative coverage and it is multiplied by -1 for interpretability.

- Trade Policy Uncertainty (TPU) Index

The Trade Policy Uncertainty (TPU) Index is originally constructed by BBVA Research based on the relative coverage associated with GDELT searches using the following set of keywords:

(tariff OR tariffs OR import OR imports OR export OR exports OR trade OR dumping OR antidumping OR GATT OR WTO) (duty OR duties OR barrier OR barriers OR ban OR bans OR tax OR taxes OR subsidy OR subsidies)

This keyword set replicates the methodology proposed by Caldara, Iacoviello, Molligo, Prestipino, and Raffo (2020) in “The Economic Effects of Trade Policy Uncertainty”.

The constructed index corresponds to the relative coverage (number of TPU-related news / total number of published news). The indices are smoothed with a 28-day moving average and normalized.

B APPENDIX B: Machine Learning Models

This appendix documents the models used in the forecasting evaluation. For each class, we summarize the functional form and the selection strategy for hyperparameters. Models are estimated on an unbalanced panel of sovereign CDS spreads, $y_{i,t+1}$, using country-level predictors $\mathbf{X}_{i,t}$. Predictors include global financial variables (U.S. 2-year yield and VIX), the Geopolitical Risk Index, local macroeconomic sentiment variables (economic and interest rate sentiment), local economic and trade uncertainty indices, and the Political Tensions Index.

B.1 Linear and Regularized Models

These models assume a linear relationship between predictors $\mathbf{X}_{i,t}$ and one-step-ahead sovereign risk $y_{i,t+1}$. Given the dimensionality of predictors and potential collinearity, we consider both OLS and regularized variants (Hastie et al., 2009). The panel has relatively few cross-sectional units (N) but a long time dimension (T), so nonlinearities are more likely to arise from temporal rather than cross-sectional complexity.

Fixed Effects OLS.

As a baseline, we estimate pooled panel regressions with country fixed effects and common slope coefficients across countries and time:

$$y_{i,t+1} = \alpha_i + \boldsymbol{\theta}^\top \mathbf{X}_{i,t} + \varepsilon_{i,t+1}, \quad (17)$$

where α_i denotes a country-specific intercept and $\boldsymbol{\theta}$ the common coefficient vector.

Lasso.

The Lasso estimator (Tibshirani, 1996) in the fixed effects setting solves

$$\hat{\boldsymbol{\theta}}^{\text{Lasso}} = \arg \min_{\boldsymbol{\theta}} \left\{ \sum_{i,t} (y_{i,t+1} - \alpha_i - \boldsymbol{\theta}^\top \mathbf{X}_{i,t})^2 + \lambda \|\boldsymbol{\theta}\|_1 \right\}. \quad (18)$$

The L1 penalty shrinks coefficients and performs variable selection. In our implementation, $\lambda = 0.001$, implying low sparsity and retention of most predictors.

Ridge.

Ridge regression (Hoerl and Kennard, 1970) with fixed effects penalizes the squared Euclidean norm of the slope vector:

$$\hat{\boldsymbol{\theta}}^{\text{Ridge}} = \arg \min_{\boldsymbol{\theta}} \left\{ \sum_{i,t} (y_{i,t+1} - \alpha_i - \boldsymbol{\theta}^\top \mathbf{X}_{i,t})^2 + \lambda \|\boldsymbol{\theta}\|_2^2 \right\}. \quad (19)$$

The estimated penalty parameter was $\lambda = 10$, consistent with substantial collinearity among predictors.

Elastic Net.

The Elastic Net (Zou and Hastie, 2005) combines the Lasso and Ridge penalties in the fixed effects model:

$$\hat{\boldsymbol{\theta}}^{\text{EN}} = \arg \min_{\boldsymbol{\theta}} \left\{ \sum_{i,t} (y_{i,t+1} - \alpha_i - \boldsymbol{\theta}^\top \mathbf{X}_{i,t})^2 + \lambda [\rho \|\boldsymbol{\theta}\|_1 + (1 - \rho) \|\boldsymbol{\theta}\|_2^2] \right\}. \quad (20)$$

Here $\rho \in [0, 1]$ controls the L1/L2 trade-off. In our setting, $\lambda = 0.01$ and $\rho = 0.1$, producing mild sparsity while preserving shrinkage.

Quantile Regression.

To capture distributional heterogeneity in CDS spreads, we estimate fixed effects quantile regressions (Koenker and Bassett, 1978). For quantile level τ :

$$Q_\tau(y_{i,t+1} | \mathbf{X}_{i,t}) = \alpha_{i,\tau} + \boldsymbol{\theta}_\tau^\top \mathbf{X}_{i,t}, \quad (21)$$

with estimator

$$(\{\hat{\alpha}_{i,\tau}\}, \hat{\boldsymbol{\theta}}_\tau) = \arg \min_{(\{\alpha_i\}, \boldsymbol{\theta})} \sum_{i,t} \rho_\tau(y_{i,t+1} - \alpha_i - \boldsymbol{\theta}^\top \mathbf{X}_{i,t}), \quad (22)$$

where $\rho_\tau(u) = u(\tau - \mathbf{1}\{u < 0\})$. We fit models at $\tau = 0.1, 0.5, 0.9$.

B.2 Principal Components Regression and Factor Models

These methods reduce the dimensionality of predictors by extracting latent components that capture most of the relevant information, mitigating multicollinearity and improving parsimony (Stock and Watson, 2003). Estimation is again based on minimizing mean squared error, but with predictors replaced by latent components.

Principal Component Regression (PCR).

PCR applies PCA to the set of regressors $\mathbf{X}_{i,t}$, retaining K components chosen via cross-validation (25 in our case). Country fixed effects are then added, and the response is regressed on the resulting scores (Jolliffe, 2002):

$$y_{i,t+1} = \alpha_i + \boldsymbol{\phi}^\top \mathbf{t}_{i,t} + \varepsilon_{i,t+1}, \quad (23)$$

where $\mathbf{t}_{i,t}$ is the K -dimensional vector of principal component scores. The estimator solves

$$\hat{\boldsymbol{\phi}} = \arg \min_{\boldsymbol{\phi}} \sum_{i,t} (y_{i,t+1} - \alpha_i - \boldsymbol{\phi}^\top \mathbf{t}_{i,t})^2.$$

Factor Analysis with Ridge (FAR).

We first extract latent factors via factor analysis,

$$\mathbf{X}_{i,t} = \Lambda f_{i,t} + \varepsilon_{i,t}, \quad \varepsilon_{i,t} \sim \mathcal{N}(0, \Psi).$$

Factor scores $\hat{f}_{i,t}$ are then used in a Ridge regression with country fixed effects:

$$\hat{\beta} = \arg \min_{\beta} \sum_{i,t} \left(y_{i,t+1} - \alpha_i - \beta^\top \hat{f}_{i,t} \right)^2 + \lambda \|\beta\|_2^2,$$

with $\lambda = 10$.

B.3 Tree-Based Ensemble Methods

Tree-based ensembles approximate complex nonlinear functions by combining the predictions of multiple decision trees. Each individual tree partitions the predictor space into regions and assigns a constant prediction within each region. Different ensemble constructions (bagging, random feature selection, boosting, or randomization of split thresholds) yield distinct bias–variance trade-offs (Hastie et al., 2009). All are trained to minimize mean squared error.

Gradient Boosting (GB).

Gradient Boosting builds an additive predictor

$$F_b(\mathbf{X}_{i,t}) = F_{b-1}(\mathbf{X}_{i,t}) + \nu f_b(\mathbf{X}_{i,t}), \quad (24)$$

where f_b is the regression tree fitted at stage b , ν the learning rate, and B the total number of boosting rounds. The final estimator is obtained by minimizing squared-error loss:

$$\widehat{F} = \arg \min_{F \in \mathcal{F}_{\text{Boost}}} \sum_{i,t} \left(y_{i,t+1} - F(\mathbf{X}_{i,t}) \right)^2. \quad (25)$$

Bagging.

Bagging averages the predictions of B bootstrap-sampled trees:

$$\hat{y}_{i,t+1}^{(\text{Bag})} = \frac{1}{B} \sum_{b=1}^B \hat{f}_b(\mathbf{X}_{i,t}), \quad (26)$$

where each base tree \hat{f}_b is trained on a bootstrap subsample \mathcal{D}_b . Each tree is estimated by

$$\hat{f}_b = \arg \min_{f \in \mathcal{F}_{\text{Tree}}} \sum_{(i,t) \in \mathcal{D}_b} \left(y_{i,t+1} - f(\mathbf{X}_{i,t}) \right)^2. \quad (27)$$

Random Forest (RF).

Random Forests extend bagging by randomly selecting m_{try} predictors at each split. The ensemble predictor is

$$\hat{y}_{i,t+1}^{(\text{RF})} = \frac{1}{B} \sum_{b=1}^B \hat{f}_b(\mathbf{X}_{i,t}), \quad (28)$$

where each tree \hat{f}_b is trained on a bootstrap sample with restricted feature sets. Formally,

$$\hat{f}_b = \arg \min_{f \in \mathcal{F}_{\text{Tree}}^{m_{\text{try}}}} \sum_{(i,t) \in \mathcal{D}_b} \left(y_{i,t+1} - f(\mathbf{X}_{i,t}) \right)^2. \quad (29)$$

In our implementation, hyperparameters were set to $n_{\text{estimators}} = 1000$, $\text{max_depth} = \text{None}$, $\text{max_features} = \text{sqrt}$, and $\text{min_samples_leaf} = 1$.

Extremely Randomized Trees (ET).

ET increase randomization by drawing split thresholds at random. The ensemble predictor is

$$\hat{y}_{i,t+1}^{(\text{ET})} = \frac{1}{B} \sum_{b=1}^B \hat{f}_b(\mathbf{X}_{i,t}), \quad (30)$$

with each tree \hat{f}_b estimated by

$$\hat{f}_b = \arg \min_{f \in \mathcal{F}_{\text{Tree}}^{\text{Rand}}} \sum_{(i,t) \in \mathcal{D}_b} (y_{i,t+1} - f(\mathbf{X}_{i,t}))^2. \quad (31)$$

Multilayer Random Forest (MLRF).

To capture heterogeneity across groups, we implement a hierarchical extension of Random Forests. In Stage 1, a forest \hat{f}_{AE} is trained on Advanced Economies (AE). In Stage 2, separate forests $\{\hat{f}_r : r \in \mathcal{R}\}$ are trained on Emerging Market (EM) regions. Prediction is piecewise:

$$\hat{y}_{i,t+1}^{(\text{MLRF})} = \begin{cases} \hat{f}_{\text{AE}}(\mathbf{X}_{i,t}) & \text{if } i \in \text{AE}, \\ \hat{f}_{\text{Region}(i)}(\mathbf{X}_{i,t}) & \text{if } i \in \text{EM}. \end{cases} \quad (32)$$

Each forest minimizes squared-error loss on its subsample:

$$\hat{f}_g = \arg \min_{f \in \mathcal{F}_{\text{RF}}} \frac{1}{n_g} \sum_{(i,t) \in \mathcal{D}_g} (y_{i,t+1} - f(\mathbf{X}_{i,t}))^2, \quad (33)$$

where $g \in \{\text{AE}\} \cup \mathcal{R}$. Equivalently, the composite loss minimized by the hierarchy is

$$\mathcal{L}_{\text{MLRF}}(\hat{f}_{\text{AE}}, \{\hat{f}_r\}) = \frac{1}{n_{\text{AE}}} \sum_{(i,t) \in \mathcal{D}_{\text{AE}}} (y_{i,t+1} - \hat{f}_{\text{AE}}(\mathbf{X}_{i,t}))^2 + \sum_{r \in \mathcal{R}} \frac{1}{n_r} \sum_{(i,t) \in \mathcal{D}_r} (y_{i,t+1} - \hat{f}_r(\mathbf{X}_{i,t}))^2. \quad (34)$$

B.4 Convolutional Neural Networks (CNNs)

Neural networks approximate nonlinear mappings by composing linear transformations with nonlinear activations. Convolutional Neural Networks (CNNs) exploit local structure in predictors using convolutional filters, pooling layers, and dense layers. For input $\mathbf{X}_{i,t} \in \mathbb{R}^p$, the prediction function is

$$\hat{y}_{i,t+1} = g_{\theta}(\mathbf{X}_{i,t}),$$

with parameters θ estimated by minimizing mean squared error:

$$\hat{\theta} = \arg \min_{\theta} \sum_{i,t} (y_{i,t+1} - g_{\theta}(\mathbf{X}_{i,t}))^2. \quad (35)$$

Shallow CNN.

A single convolutional layer with ReLU activation, followed by max pooling, flattening, and a dense hidden layer. This setup captures simple localized interactions between predictors.

Deep CNN.

Two convolutional blocks with ReLU activations, pooling, and dropout for regularization, followed by dense layers. Hyperparameters (filters, kernel size, hidden units, dropout rates) are tuned by random search with KerasTuner (O’Malley et al., 2019), minimizing validation MSE.